POLITECNICO DI TORINO
Repository ISTITUZIONALE

Microcanonical ensemble out of equilibrium

Original
Microcanonical ensemble out of equilibrium / Belousov, R., Elliott, J., Berger, F., Rondoni, L., Erzberger, A.. - In: PHYSICAL REVIEW. E. - ISSN 2470-0045. - STAMPA. - 113:1(2026), pp. 1-20. [10.1103/r1cg-tpdb]

Availability:
This version is available at: 11583/3010697 since: 2026-05-09T17:48:53Z

Publisher:
American Physical Society - APS

Published
DOI:10.1103/r1cg-tpdb

Terms of use:

This article is made available under terms and conditions as specified in the corresponding bibliographic description in the repository

Publisher copyright

(Article begins on next page)

25 November 2026

Microcanonical ensemble out of equilibrium

R. Belousov [1,*] J. Elliott [1,2] F. Berger [3] L. Rondoni [4,5] and A. Erzberger [1,2,†]

[1]*Cell Biology and Biophysics Unit, European Molecular Biology Laboratory, Meyerhofstraße 1, 69117 Heidelberg, Germany*

[2]*Department of Physics and Astronomy, Heidelberg University, 69120 Heidelberg, Germany*

[3]*Cell Biology, Neurobiology and Biophysics, Department of Biology, Faculty of Science, Utrecht University, 3584 Utrecht, The Netherlands*

[4]*Department of Mathematical Sciences, Politecnico di Torino, Corso Duca degli Abruzzi 24, 10129 Turin, Italy*

[5]*INFN, Sezione di Torino, 10125 Turin, Italy*

(Received 30 May 2025; revised 6 November 2025; accepted 2 January 2026; published 23 January 2026)

Introduced by Boltzmann under the name "monode," the microcanonical ensemble serves as the fundamental representation of equilibrium thermodynamics in statistical mechanics by counting all possible realizations of a system's states. Ensemble theory connects this idea with probability and information theory, leading to the notion of Shannon-Gibbs entropy and, ultimately, to the principle of maximum caliber describing *trajectories* of systems—in and out of equilibrium. While the latter phenomenological generalization reproduces many results of nonequilibrium thermodynamics, given a proper choice of observables, its physical justification remains an open area of research. What is the microscopic origin and physical interpretation of this variational approach? What guides the choice of relevant observables? We address these questions by extending Boltzmann's method to a microcanonical caliber principle and counting realizations of a system's trajectories—all assumed equally probable. Maximizing the microcanonical caliber under the imposed constraints, we systematically develop generalized local detailed-balance relations, clarify the statistical origins of inhomogeneous transport, and provide an independent derivation of key equations from stochastic thermodynamics. This approach introduces a *dynamical* ensemble theory for nonequilibrium steady states in spatially extended and active systems. While verifying the equivalence of ensembles, e.g., those of Norton and Thévenin, our framework contests other common assumptions about nonequilibrium regimes, with supporting evidence provided by stochastic simulations. Our theory suggests further connections to the first principles of microscopic dynamics in classical statistical mechanics, which are essential for investigating systems where the necessary conditions for thermodynamic behavior are not satisfied.

DOI: 10.1103/r1cg-tpdb

I. INTRODUCTION

Tools of statistical mechanics have become indispensable in addressing modern problems of science and technology, which concern complex, active, and, in general, far from equilibrium systems [1–25]. These tools extend, typically in a phenomenological manner, classical results for equilibrium thermodynamic systems, e.g., local detailed-balance relations [26–28], statistics of large deviations, information [29–34] and response theory [35–37]. The assumptions implied in such extensions are difficult to validate and, when not verified, drastically limit applications or physical interpretation of theoretical models. To overcome the limitations of phenomenological approaches to nonequilibrium thermodynamics, the search for generalizations of the principles, which statistical mechanics established for equilibrium systems—ensemble methods [38,39], Helmholtz' mechanical interpretation [40,41], and dynamical-systems theory [42–48]—continues.

The ensemble theory of statistical mechanics [49,50] provides the most widely adopted framework of thermodynamics, which relates macroscopic properties of *equilibrium systems* to time-independent statistics of their micro- or mesoscopic states $\boldsymbol{s} \in \boldsymbol{\sigma}$, e.g., positions and momenta of all the particles or occupation numbers of energy levels. Dynamical fluctuations in these systems are thus characterized by the probability distribution $p_\sigma(\boldsymbol{s})$, which does not change in time, because any macroscopic variable $\langle A(\boldsymbol{s})\rangle = \int_{\boldsymbol{\sigma}} \boldsymbol{ds}\, p_\sigma(\boldsymbol{s}) A(\boldsymbol{s})$ must by definition remain constant in equilibrium. According to statistical mechanics, the distribution $p_\sigma(\boldsymbol{s})$ maximizes the Gibbs entropy defined as

$$S_\sigma = -k_{\mathrm{B}} \int_{\boldsymbol{\sigma}} \boldsymbol{ds}\, p_\sigma(\boldsymbol{s}) \ln p_\sigma(\boldsymbol{s}), \tag{1}$$

where the Boltzmann constant, $k_{\mathrm{B}} = 1.380649 \times 10^{-23}\,\mathrm{J}/K$, has units of entropy and quantifies the vast disparity of scales between the macroscopic and the microscopic realms. In systems with discrete sets of states, the integral is replaced by the summation.

If one does not speak of the thermodynamic entropy, which is an objective function of a macroscopic state, then S_σ/k_{B} can

*Contact author: roman.belousov@embl.de

†Contact author: erzberge@embl.de

Published by the American Physical Society under the terms of the Creative Commons Attribution 4.0 International license. Further distribution of this work must maintain attribution to the author(s) and the published article's title, journal citation, and DOI.

be interpreted as a measure of indeterminacy. In this context, it is commonly referred to as Shannon entropy, a subjective quantity that depends on the level of system description. For instance, a level of uncertainty can be intentionally introduced through coarse graining [51,52], as suitable in some applications [53,54].

As an extension of the information-theoretic approach from time-independent macroscopic states to general dynamical processes, the principle of maximum caliber was coined by Jaynes [55], although its foundations go back to much earlier works of his [56], as well as of Filyukov and Karpov [57,58]. If we assign probabilities $p_{\mathcal{T}}(\boldsymbol{s}_t)$ to the possible trajectories $\boldsymbol{s}_t$—a time-ordered succession of states—of a system, then its caliber or *path* entropy over the interval $t \in \mathcal{T}$ mimics Eq. (1) as

$$S_{\mathcal{T}} = -\int_{\sigma\times\mathcal{T}} \mathcal{D}\boldsymbol{s}_t \, p_{\mathcal{T}}(\boldsymbol{s}_t) \ln p_{\mathcal{T}}(\boldsymbol{s}_t), \tag{2}$$

with the integral taken over all possible paths s_t. According to the principle of maximum caliber or path entropy,[1] which is thought to be applicable also out of equilibrium [28,32,38,55,57–59,61–80], the probability distribution $p_{\mathcal{T}}(\boldsymbol{s}_t)$ is identified by extremizing Eq. (1) subject to known macroscopic constraints (Appendix A).

Despite the mathematical analogy shared by Eqs. (1) and (2), the principle of maximum caliber still lacks the foundations that are well established and understood within the context of maximum-entropy principle for equilibrium systems, whose relevant variables and constraints are known [81]. In particular, a complete picture of nonequilibrium statistics—the mathematical derivation and its physical interpretation based on the dynamics of microscopic constituents of matter [82]—is so far missing. Statistical mechanics encompasses the relevant macroscopic constraints that the equilibrium ensembles must verify, consistently with Liouville's theorem and Hamiltonian dynamics [83, Chapter 2]. Consequently, statistics of equilibrium systems can be derived from the microscopic representation of these constraints within the microcanonical ensemble [83, Chapter 3], [84].

When maximizing the system's caliber, the choice of the macroscopic constraints is typically guided by phenomenological laws of nonequilibrium thermodynamics. Thereby the selected variables often include—in addition to properties whose relevance is well established from the equilibrium theory, like energy and mass—phenomenological parameters such as the magnitudes of currents. However the distinction between these types of variables is not always appreciated and may lead to an inadequate, or valid only in a certain limit, description.

Even for nonequilibrium steady states—regimes formally similar to equilibrium, because they are characterized by constant nonzero fluxes—there is no universally accepted choice of the macroscopic statistics. Variants of the maximum-caliber formalism differ by imposed constraints or by the way interactions with thermodynamic reservoirs are modeled [58,71–74,85–87]. In fact, as we find here, even the commonly invoked condition of a constant macroscopic flux can arise from different physical mechanisms, leading to distinct nonequilibrium regimes.

Especially when multiple constraints must be chosen to describe a complex system, physical insights are in high demand. For example, which macroscopic observables would provide the relevant statistics for nontrivial spatial organization—such as gradients of chemical components or patterns in living systems—that shapes important processes in biology and engineering [88–93]? This question leads us to consider also applications of the maximum-caliber principle to systems whose thermodynamic variables can be regarded as fields. In particular, we show how the symmetry broken by nonequilibrium mechanisms entails a spatial gradient of matter.

To develop the ensemble representation for systems beyond the scope of classical equilibrium thermodynamics, we combine *some* ideas of the caliber theory [66] with the microcanonical approach, starting from Boltzmann's simplified model of an ideal gas [94]. We proceed by counting all possible microscopic trajectories of a system—assumed equally likely—rather than its microscopic states as in Boltzmann's original method. The macroscopic evolution of the system is then identified with its most probable path that maximizes the number of such realizations.

Subsequently, we extend our theory to more complex systems in and out of equilibrium, by incorporating more realistic dynamical constraints, which introduce interactions between the microscopic constituents of matter, ensure the continuity of its flow, or apply driving forces. In the outcome we systematically obtain by direct calculations a physically interpretable, mechanistic representation of thermodynamic ensembles for spatially extended, nonequilibrium, and active systems, which we ultimately verify in stochastic simulations.

The connection to microscopic events offers the physical insight, which is missing in the formal variational principles, and a systemetic way to complete statistical-mechanics models with conjugate pairs of thermodynamic variables suitable to describe specific nonequilibrium regimes. These variables uniquely identify the statistical ensemble, which turns out to depend not only on the magnitude and direction of the currents, e.g., as assumed in the typical phenomenological theories, but on the details of the driving mechanism.

The distinct features of our theory comprise the microcanonical constraints and *local*, in time, analysis of trajectories. First, we impose conservation of the total energy E and the number of particles N in the system—regardless of any nonequilibrium driving $\boldsymbol{\Theta}$, such as fixed currents or difference of thermodynamic potentials that may be present. Second, we count the realizations of the trajectories over a short, or rather infinitesimal, time step of size dt. Under these conditions we replace Eqs. (1) and (2) with their microcanonical counterparts—the Boltzmann entropy $S_{\mathrm{B}} = k_{\mathrm{B}} \ln W(N, E)$ (Appendix B) and *microcanonical caliber* (*microcaliber*)

$$S_{dt} = \ln \Omega(E, N, \boldsymbol{\Theta}\ldots), \tag{3}$$

where W and Ω count the realizations of the system's macroscopic states and trajectories, respectively.

Maximization of the microcanonical caliber subtly differs from the nonlocal—*in time*—variational problem formulated as the global optimum of the traditional path entropy over the

[1] Or second entropy [59,60].

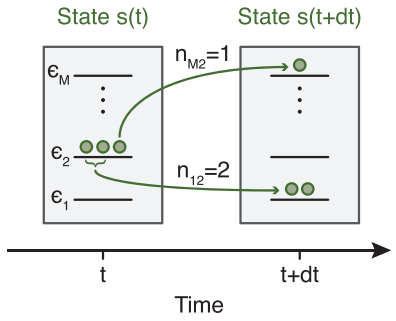

FIG. 1. Simplified model of ideal gas. In the initial state $\boldsymbol{s}(t)$ indistinguishable particles are distributed over M energy levels $\epsilon_{i=1,2,\ldots,M}$. In each discrete time step dt, n_{ji} particles move from the ith to the jth level, with n_{ii} particles remaining in their place.

interval $\mathcal{T}$. The time-nonlocal approach identifies the most likely evolution of a system by extremizing the functional Eq. (2), which in continuum problems typically entails the conditions for extrema at each instant of time as well (Appendix C), like the Euler-Lagrange equations minimizing the action functional in the classical mechanics. Therefore our microcanonical formalism is compatible with the traditional principle of maximum caliber defined for paths over a macroscopic observation times $\mathcal{T}$.

II. PARADIGMATIC MODELS

First we develop and demonstrate our theoretical framework using two paradigmatic models of classical statistical mechanics. We begin with the Boltzmann gas, representing the simplest class of problems considered, and then proceed to the Fermi gas, which illustrates nontrivial effects of microscopic interactions.

A. Boltzmann gas

To introduce the microcaliber theory in the simplest form, we begin with Boltzmann's paradigmatic model of an ideal gas in discrete time t and state space $\boldsymbol{\sigma}$ (Fig. 1): N indistinguishable particles may occupy any of $M \gg N$ energy levels $\epsilon_{i=1,2,\ldots,M}$ with degeneracies g_i. The system's state can thus be described by a vector of occupation numbers $\boldsymbol{s} = (n_1, n_2, \ldots, n_M)^{\mathrm{T}} \in \boldsymbol{\sigma}$.

Starting with an arbitrary initial state—not necessarily fulfilling the maximum-entropy condition (Appendix B)—and implementing the microcanonical conditions, we impose a *macroscopic constraint* on the total energy, $E = \sum_i \epsilon_i n_i$, which must be conserved in time, and a single *microscopic constraint* on the dynamics—particles are neither created nor annihilated. They are however allowed to move to, or remain still in, any energy level, as long as in a time step $t \to t + dt$ the transition between two states $\boldsymbol{s}, \boldsymbol{s}' \in \boldsymbol{\sigma}$, obeys $N(\boldsymbol{s}) = N(\boldsymbol{s}')$ and $E(\boldsymbol{s}) = E(\boldsymbol{s}')$. How many distinct realizations of such a transition are possible?

Given the above conditions, any transition $\boldsymbol{s}_{dt} : \boldsymbol{s} \to \boldsymbol{s}'$—or the system's *path*—can be uniquely specified by the set $\{n_{ji}\}_{i,j=1}^{M}$ of numbers of particles, which jump from the ith level into the jth level. The elements n_{ji} must satisfy the following relations:

$$n_i(t) - \sum_{j=1}^{M} n_{ji} = 0, \quad n_j(t+dt) - \sum_{i=1}^{M} n_{ji} = 0, \tag{4}$$

$$0 = \sum_{ij} (\epsilon_i - \epsilon_j) n_{ji} = E - \sum_j \epsilon_j n_j(t+dt), \tag{5}$$

which enforce the conservation of the total number of particles and their total energy, counting also those that remain at the same level, $i = j$.

Each of the elements n_{ji}—which together define a path of the system—represents the number of particles taken from the state i and redistributed independently over g_j sublevels of energy ϵ_j. The total count of indistinguishable particles' rearrangements is approximately given by the classical combinatorial formula of the Maxwell-Boltzmann statistics[2] $\Omega_{ji} \approx g_j^{n_{ji}}/n_{ji}!$ [95, Chapter 13]. As the particles are distributed independently, the number of realizations of the system's path $\{n_{ji}\}_{i,j=1}^{M}$ amounts to

$$\Omega_{\mathrm{MB}}(\boldsymbol{s}_{dt}) = \prod_{i,j=1}^{M} \Omega_{ji} \approx \prod_{i,j=1}^{M} \frac{g_j^{n_{ji}}}{n_{ji}!}. \tag{6}$$

Assuming that all rearrangements of particles are equally likely, the most probable path of the system is characterized by the largest number of realizations, which is an objective quantity. It is given by the n_{ji} that maximize the logarithm of Eq. (6)—*the microcanonical caliber of the path*—together with the explicit constraints on the particles' number and their energy. The corresponding objective function we extremize is

$$f_{\mathrm{MB}} = \ln \Omega_{\mathrm{MB}} + \beta \left(E - \sum_{ij} \epsilon_j n_{ji} \right) + \sum_i \theta_i \left(n_i - \sum_j n_{ji} \right), \tag{7}$$

where the Lagrange multipliers β and $\theta_{i=1,2,\ldots,M}$ constrain the total energy E and the initial occupation numbers $n_i(t)$, respectively. By applying the Stirling approximation to the microcanonical caliber

$$S_{dt} = \ln \Omega_{\mathrm{MB}} \approx \sum_{ij} [n_{ji} \ln g_j - n_{ji}(\ln n_{ji} - 1)], \tag{8}$$

and the extremum condition $\partial f_{\mathrm{MB}}/\partial n_{ji} = 0$, we find

$$n_{ji} = g_j e^{-\beta \epsilon_j - \theta_i}. \tag{9}$$

The constraint Eq. (4) on $n_i(t)$ determines values of the Lagrange multipliers θ_i:

$$e^{-\theta_i} = \frac{n_i}{Z_{\mathrm{MB}}}, \tag{10}$$

[2]The Maxwell-Boltzmann combinatorial formula may be regarded as an approximation of the Bose-Einstein statistics when $M \gg N$ and differs from the Boltzmann's exact counting of distinguishable particles by the factor of $n_i!$ [95, Chapter 13].

in which $Z_{\mathrm{MB}} = \sum_j g_j \exp(-\beta\epsilon_j)$ is the canonical partition function. Combined, Eqs. (9) and (10) yield

$$n_{ji} = \frac{g_j}{Z_{\mathrm{MB}}} e^{-\beta\epsilon_j} n_i = g_j \pi_{ji} n_i = p_{ji} n_i, \tag{11}$$

where the elements $\pi_{ji} = \exp(-\beta\epsilon_j)/Z_{\mathrm{MB}}$, which in this simple model do not actually depend on the index i, express the probability for a particle to jump from an ith energy level into *one* of the g_j equivalent sublevels of energy ϵ_j. In addition, we can define the probability $p_{ji} = g_j \pi_{ji}$ for a particle to jump into *any* of the degenerate sublevels j. Note here that π_{ji} satisfy the simplest form of local detailed balance, whereas p_{ji} obey a more general relation:

$$\frac{\pi_{ji}}{\pi_{ij}} = e^{-\beta(\epsilon_j - \epsilon_i)}, \quad \frac{p_{ji}}{p_{ij}} = \frac{g_j}{g_i} e^{-\beta(\epsilon_j - \epsilon_i)}. \tag{12}$$

Using the above results and definitions, we can use the constraint Eq. (4) on $n_j(t + dt)$ as a Markov-chain equation for the most likely evolution—the macroscopic path—of the system:

$$n_j(t + dt) = \sum_i p_{ji} n_i(t). \tag{13}$$

Due to the local detailed-balance relations (12), the system will reach a steady state $\bar{n}_j = n_j(\infty)$ as $t \to \infty$:

$$\bar{n}_j = \sum_i p_{ji} \bar{n}_i = g_j e^{-\beta\epsilon_j} \frac{N}{Z_{\mathrm{MB}}} = g_j e^{\beta(\mu_{\mathrm{MB}} - \epsilon_j)}, \tag{14}$$

which is the distribution of the microcanonical equilibrium ensemble with inverse temperature $\beta = (k_{\mathrm{B}}T)^{-1}$ and chemical potential $\mu_{\mathrm{MB}} = -k_{\mathrm{B}}T \ln(Z_{\mathrm{MB}}/N)$, cf. Eq. (B1) in Appendix B.

Instead of maximizing the Boltzmann entropy (Appendix B), we derived the distribution function Eq. (14) of the microcanonical ensemble alongside the Markovian macroscopic dynamics Eq. (13), which encompasses the transient relaxation of any initial state $n_i(t)$ to equilibrium $\bar{n}_i(\infty)$. This theory can also be extended to continuous-time random walks in a straightforward manner, by casting Eq. (13) as a master equation (Appendix D) in the limit of $dt \to 0$ with transition rates

$$k_{ji} = \lim_{dt \to 0} \frac{p_{ji}}{dt}. \tag{15}$$

The limit $dt \to 0$ in the above equation refers to infinitesimal variations relative to macroscopic timescales. Specifically in the discrete-time model of the Boltzmann gas we regard the Markov chain Eq. (13) as an approximation of a time-continuous process with a Poissonian *attempt* rate $a = dt^{-1}$ [96], such that $k_{ij} = a p_{ij}$ and, thus, $p_{ij} \simeq k_{ij} dt$ [97, Sec. 2.3].

In the rest of the paper, we consider increasingly more complex microscopic constraints, which incorporate various important aspects of real physical systems neglected in the paradigmatic example of this section. Further developments follow relying as above on the maximization of the discrete microcanonical *caliber* S_{dt}, here taking the form of $S_{dt} = \ln \Omega_{\mathrm{MB}}(\boldsymbol{s}_{dt})$.

B. Fermi gas

Although quantum physics is beyond the scope of this paper, we consider the exclusion principle—leading to Fermi-Dirac statistics [95, Chapter 13]—as a paradigmatic example of steric interparticle interactions in classical thermodynamic systems. Namely, we forbid two or more particles to occupy the same sublevel of a given energy ϵ_i. This condition restricts the maximum occupation number of an ith level by its degeneracy $n_i \leqslant g_i$. Indeed, besides fermions in quantum physics, a variant of the exclusion principle often appears in models of classical statistical mechanics as a simplified representation of hard-core repulsion, e.g., in Flory-Huggins solution theory [98–100], [101, Section 1.4] or lattice Boltzmann methods [102,103]. When the degeneracy of an energy level is associated with the spatial localization of its sublevels, this type of interaction results in volume exclusion [104–109]. Such a situation may describe a collection of particles and boxes too small to host more than one particle. The Fermi-Dirac distribution arises through maximization of the Boltzmann entropy at constant number of particles and constant energy, by using the Stirling approximation.[3]

As in Sec. II A the system's trajectory $\boldsymbol{s}_{dt}$ over a time step dt is completely specified by its elements n_{ji}. However, while the particles are allowed to jump into any level (Fig. 1), in addition to constraints (4) and (5), the exclusion principle demands

$$n_i(t) = \sum_j n_{ji} \leqslant g_i, \quad n_j(t + dt) = \sum_i n_{ji} \leqslant g_j. \tag{16}$$

With the above listed assumptions, counting realizations of a path subject to the constraints (16) leads to a formula of the system's caliber that resembles the Fermi-Dirac statistics (Appendix E):

$$\Omega_{\mathrm{FD}}(\boldsymbol{s}_{dt}) = \prod_j \frac{g_j!}{(g_j - \sum_i n_{ji})! \prod_i n_{ji}!}. \tag{17}$$

By maximizing $\ln \Omega_{\mathrm{FD}}$ with Lagrange multipliers β and θ_i to the constraint Eqs. (4) and (5) we further obtain (Appendix E)

$$n_{ji} = \frac{g_j - n'_j}{Z_{\mathrm{FD}}} e^{-\beta\epsilon_j} n_i = p_{ji} n_i, \tag{18}$$

where we used for brevity $n'_j = n_j(t + dt)$ and, as in Sec. II A, the transition probabilities p_{ji}, which depend on the Fermi-Dirac partition function $Z_{\mathrm{FD}} = \sum_j (g_j - n'_j) \exp(-\beta\epsilon_j)$. From the constraint Eq. (4) on $n'_j = \sum_i n_{ji}$ we again obtain a Markov chain

$$n_j(t + dt) = \sum_i p_{ji} n_i(t),$$

[3]The Stirling approximation requires both the number of particles in a given energy level n_i, as well as the number of unoccupied sublevels $g_i - n_i$ to be sufficiently large. Nonetheless, despite its asymptotic nature, the error in Stirling's approximation is generally negligible on macroscopically relevant scales, even for small positive integers.

whose steady state must satisfy the equation

$$\bar{n}_j = \sum_i p_{ji}\bar{n}_i = \frac{g_j - \bar{n}_j}{Z_{\rm FD}} e^{-\beta\epsilon_j} N. \tag{19}$$

The solution of Eq. (19) is the equilibrium Fermi-Dirac distribution with the chemical potential $\mu_{\rm FD} = -k_{\rm B}T \ln(Z_{\rm FD}/N)$:

$$\bar{n}_j = \frac{g_j}{1 + e^{\beta(\epsilon_j - \mu_{\rm FD})}}. \tag{20}$$

Note that the microcaliber theory imposes a general condition on the transition probabilities p_{ji}:

$$\frac{p_{ji}(g_i - n_i(t+dt))}{p_{ij}(g_j - n_j(t+dt))} = e^{-\beta(\epsilon_j - \epsilon_i)}, \tag{21}$$

which in equilibrium reduces to that of the local detailed balance for fermions [110,111]

$$\frac{p_{ji}(g_i - \bar{n}_i)}{p_{ij}(g_j - \bar{n}_j)} = e^{-\beta(\epsilon_j - \epsilon_i)}. \tag{22}$$

The Fermi gas example shows how the microcanonical principle of maximum caliber reproduces the classical results of statistical mechanics for such systems, e.g., Eqs. (20) and (22), and provides their nonequilibrium generalizations, e.g., Eq. (21) and those derived in the following. Interactions more complex than the Fermi exclusion principle can also be taken into account (Appendix F, Ref. [109]).

III. SPATIALLY EXTENDED SYSTEMS

De Groot and Mazur [112, Chapter I, Sec. 2] argue in their, now classical, book on nonequilibrium thermodynamics, which they regard in connection to such macroscopic disciplines as fluid dynamics and electromagnetic theory, that "*the thermodynamics of irreversible processes should be set up from the start as a continuum theory, treating the state parameters of the theory as field variables...*"

To pursue the idea of formulating a macroscopic theory for field variables, we first reframe the Boltzmann model of the ideal gas (Sec. II A) using discretized field variables on a lattice. Then we analyze its thermodynamics in and out of equilibrium by applying the microcanonical principle of maximum caliber, and ultimately taking the continuum limit in space.

A. Boltzmann gas on a periodic lattice

More realistic representations of macroscopic systems can be achieved by associating energy levels with sites on a lattice, e.g., on an equidistant grid of size dx which in the continuum limit $dx \to 0$ yields a field description extended over the coordinate x (Appendix G). For example, such lattice sites may correspond to coarse-grained positions of molecules in space (Fig. 2). Here we consider the Boltzmann gas with energy sets $\epsilon_i(\ell)$ with $i = 1, \ldots, M(\ell)$ and $\ell = 1, 2, ..., L$, and degeneracies $g_i(\ell)$, where the index ℓ refers to an ℓth site. Thereby the system represents a (quasi-) one-dimensional system with particles' energy states localized in space. In addition, we impose periodic boundary conditions.

We introduce a new constraint on the microscopic dynamics, which corresponds to the continuity conditions of

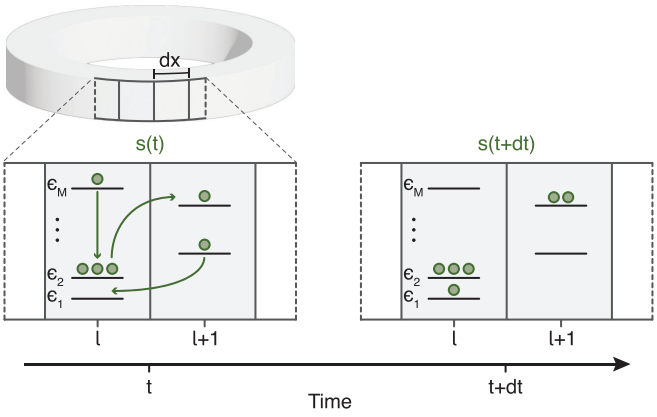

FIG. 2. Boltzmann gas on a lattice of length scale dx with periodic boundary conditions. In general the structure of energy levels $\epsilon_i(\ell)$ with $i = 1, \ldots, M(\ell)$ and $\ell = 1, 2, ..., L$, is different at each site of the lattice. In a time step dt particles are allowed to jump only between the levels of the same site ℓ or of its nearest neighbors $\ell \pm 1$.

continuum fields, and which restricts possible transitions from a source level $\epsilon_i(\ell)$ to the target levels $\epsilon_j(m \in \mathcal{N}(\ell))$ within the *neighborhood* $\mathcal{N}(\ell)$ of the ℓth site. We take the simplest such neighborhood $\mathcal{N}(\ell) = \{\ell - 1, \ell, \ell + 1\}$ with periodic boundary conditions $\mathcal{N}(1) = \{L, 1, 2\}$ and $\mathcal{N}(L) = \{L - 1, L, 1\}$.

Using two indices, instead of one, to enumerate the energy levels does not change much in the framework outlined in Sec. II. In fact, double indexing can be in practice "flattened out," given a finite set $i \in \mathcal{M}(\ell) = \{1, 2, ..., M_\ell\}$ of energy levels $\epsilon_i(\ell)$ per site ℓ. Hence the count of realizations of a path specified by $n(mj|\ell i)$—the number of particles transferred between the source and target levels $\epsilon_i(\ell)$ and $\epsilon_j(m)$, respectively—is still given by the Maxwell-Boltzmann statistics

$$\Omega_0(\boldsymbol{s}_{dt}) \approx \prod_{\substack{\ell=1 \\ i\in\mathcal{M}(\ell)}}^{L} \prod_{\substack{m\in\mathcal{N}_\ell \\ j\in\mathcal{M}(m)}} \frac{g_j(m)^{n(mj|\ell i)}}{n(mj|\ell i)!}, \tag{23}$$

cf. Eq. (6). We also impose the constraints

$$A_{\ell i} = n_i(\ell, t) - \sum_{m\in\mathcal{N}(\ell),\, j\in\mathcal{M}(m)} n(mj|\ell i) = 0, \tag{24}$$

$$B = E - \sum_{\substack{\ell=1,m=\ell-1 \\ i\in\mathcal{M}(\ell),\, j\in\mathcal{M}(m)}}^{L,\ell+1} \epsilon_j(m) n(mj|\ell i) = 0, \tag{25}$$

subject to the periodic boundary conditions $n_i(L+1) = n_i(1)$, thus applying the condition of conservation of number of particles and energy expressed by Eqs. (4) and (5) to the case of transitions from a given source level to a neighborhood $\mathcal{N}(\ell)$. Next, to maximize the system's caliber, we form the objective function

$$f_0 = \ln \Omega_0(\boldsymbol{s}_{dt}) + \beta B(\boldsymbol{s}_{dt}) + \sum_{\ell i} \theta_{\ell i} A_{\ell i}(\boldsymbol{s}_{dt}), \tag{26}$$

with the Lagrange multipliers $\theta_{\ell i}$ and β to the constraints (24) and (25), respectively. We do not repeat here the steps of Sec. II A required to extremize f_0 and to eliminate $\theta_{\ell i}$, and

write immediately the final result for the most likely path of the system

$$n(mj|\ell i) = \frac{g_j(m)}{\zeta(\ell)} e^{-\beta\epsilon_j(m)} n_i(\ell) = p(mj|\ell i) n_i(\ell), \tag{27}$$

in which we introduced a *neighborhood* partition function

$$\zeta(\ell) = \sum_{m\in\mathcal{N}(\ell),\, j\in\mathcal{M}(m)} g_j(m) e^{-\beta\epsilon_j(m)},$$

and the transition probabilities $p(mj|\ell i)$, with $m \in \mathcal{N}_\ell$. The latter can be augmented by elements $p(m \notin \mathcal{N}(\ell),\, j|\ell i) = 0$ to cast a Markov chain equation, cf. Eq. (13),

$$n_j(m, t + dt) = \sum_{\ell i} p(mj|\ell i) n_i(\ell), \tag{28}$$

in which we observe another generalization of the local detailed-balance relation

$$\frac{p(mj|\ell i)}{p(\ell i|mj)} = \frac{g_j(m)\zeta(\ell)}{g_i(\ell)\zeta(m)} e^{-\beta(\epsilon_j(\ell)-\epsilon_i(m))}, \tag{29}$$

when $m \in \mathcal{N}(\ell)$. In a uniform system with $\zeta(m) = \zeta(\ell)$ and $g_j(m) = g_i(\ell)$ this relation simplifies to the more common form.

The equilibrium state corresponds to the steady-state solution of Eq. (28):

$$\bar{n}_j(m) = \sum_{\ell i} p(mj|\ell i)\bar{n}_i(\ell) = \frac{g_j(m)}{e^{\beta\epsilon_j(m)}} \sum_{\ell\in\mathcal{N}(m)} \frac{\bar{\nu}(\ell)}{\zeta(\ell)}, \tag{30}$$

where $\nu_\ell = \sum_i n_i(\ell)$ counts the particles at the site ℓ. This linear equation can be solved explicitly, once the structures of energy levels—how $g_i(\ell)$ and $\epsilon_i(\ell)$ depend on the indices i and ℓ—are defined. Inhomogeneous structures are possible, e.g., in the presence of external forces like gravity. In the absence of such forces the equilibrium solution manifests the macroscopic symmetry, which demands that all sites, as they are equivalent, are characterized by the same numbers

$$\bar{\nu}(\ell) \equiv \frac{N}{L}, \quad \zeta(\ell) \equiv 3z = 3\sum_j g_j e^{-\beta\epsilon_j}, \tag{31}$$

where we drop the dependence of g_j and ϵ_j on the index m. The factor of 3 appears from expansion of the neighborhood partition function ζ comprising contributions of the local partition function z from three identical lattice sites. Equation (31) substituted into (30) reproduces the macroscopic statistics Eq. (14) for the Boltzmann gas:

$$\bar{n}_j(m) = g_j e^{\beta(\mu_{\rm MB}-\epsilon_j)}, \tag{32}$$

in which the chemical potential at each site is given by

$$\mu_{\rm MB} = k_{\rm B}T \ln \frac{3N/L}{3z} = -k_{\rm B}T \ln \frac{Z_{\rm MB}}{N}, \tag{33}$$

with $Z_{\rm MB} = Lz$ being the macroscopic partition function.

The microcanonical principle of maximum caliber, as shown above, encompasses the Markovian dynamics Eq. (28), which describes the decay of the transients toward the equilibrium states. Thereby this approach consistently extends the ensemble formalism of classical statistical mechanics. In addition to the continuous-time limit, mentioned in Sec. II A and leading to the master equation (Appendix D), the lattice representation connects the microcanonical principle of maximum caliber to the field theories through the continuum limit of $dx \to 0$ (Appendix G).

B. Gradient-driven flow

Steady states with constant macroscopic flows, which are sustained by external gradients of thermodynamic potentials, represent the classical subject of nonequilibrium thermodynamics, cf. Ref. [112, Chapter V] and Ref. [60, Sec. 1.5]. Here we show how the microcaliber framework can be applied to analyze statistical mechanics of such systems.

Extending the ideal-gas model on a lattice from Sec. III A, we drive the system out of equilibrium by imposing a macroscopic constraint enforcing a constant flux of particles J between the end sites $\ell = 1, L$:

$$P_{1L}(s_{dt}) = J - \sum_{ij} [n(1\,j|Li) - n(Lj|1i)] = 0, \tag{34}$$

which implies $J > 0$ when the particles are driven counterclockwise in Fig. 2. Note that this constraint is *not* equivalent to constant flux in the whole system, as clarified in the next section.

The nonequilibrium mechanism we thus describe resembles closing an electric circuit by connecting its ends to positive and negative terminals of a "battery." Then, by adding the additional constraint P_{1L} with a new Lagrange multplier η_{1L} to Eq. (26), we extremize the objective function

$$f_{1L} = f_0 + \eta_{1L} P_{1L}. \tag{35}$$

For $m, \ell \notin \{1, 2, L-1, L\}$ we obtain again Eq. (27), as these sites are not affected by the new constraint. The explicit expressions for the affected sites, which involve the Lagrange multiplier η_{1L}, are derived in Appendix H [Eqs. (H6) and (H7)].

The dynamics of the system can be cast as Eq. (28) by using Eqs. (27), (H6)–(H7), like in Sec. III A. Due to the constant-flux condition, its steady-state solution $\bar{n}_i$ must obey Kirchhoff's law:

$$J_{\ell+1,\ell} = \sum_{ij} [n(\ell+1,\, j|\ell i) - n(\ell,\, j|\ell+1,\, i)] = J. \tag{36}$$

Now we focus on a subsystem consisting of sites $\ell \in S_0 = \{a, a+1, ..., b\}$ with $a \gg 1$ and $b \ll L$. The complementary subsystem $\ell \in \bar{S}_0 = \{b+1, b+2, ..., a-1\}$, internally connected through the periodic boundary conditions, plays the role of a *nonequilibrium* reservoir.

In the subsystem of interest S_0, Eq. (36) can be evaluated with help of Eq. (27):

$$J_{\ell+1,\ell}(S_0) = \frac{z(\ell+1)}{\zeta(\ell)}\bar{\nu}(\ell) - \frac{z(\ell)}{\zeta(\ell+1)}\bar{\nu}(\ell+1),$$

which for the Boltzmann gas with homogeneous structure of energy levels reduces to

$$J_{\ell+1,\ell}(S_0) = -\frac{z}{\zeta}\Delta\bar{\nu}(\ell) = -\frac{1}{3}\Delta\bar{\nu}(\ell) = J,$$

with the forward difference $\Delta\bar{\nu}(\ell) = \bar{\nu}(\ell+1) - \bar{\nu}(\ell)$. Hence, the steady state characterized by the constraint (34) induces a

constant gradient of matter in the opposite direction of the flux it sustains within the bulk of the system.

If we assume that the complementary system $\bar{S}_0$ acts as a perfect reservoir, then it can be eliminated from the model by imposing on the subsystem of interest S_0 constant boundary conditions $\nu(\ell \in \{a-1, b+1\}) = \bar{\nu}(\ell)$ at the sites $a-1$ and $b+1$. In principle, given the fixed number of bins and the energy levels' structure, the Lagrange multiplier $\eta(J)$ and the gradient it induces can be evaluated at least numerically.

At the level of the whole system, the nonequilbrium steady state is sustained by a pair of asymmetric *active exponents* $\phi_{1L} = -\phi_{L1} = -\eta_{1L}$ introduced in Ref. [96, Supplemental Material Sec. 2] and discussed in Appendixes H and I. They break the equilibrium detailed-balance relation for the transition rates and, instead of Eq. (29), yield

$$\frac{p(Lj|1i)}{p(1j|Li)} = \frac{g_j(L)\zeta_\phi(1)}{g_i(1)\zeta_\phi(L)} e^{-\beta\left(\epsilon_j(\ell)-\epsilon_i(m)\right)+\Delta\phi}, \tag{37}$$

where $\Delta\phi = \phi_{1L} - \phi_{L1} = -2\eta_{L1}$ and $\zeta_\phi(\ell \in \{1, L\})$ is the *extended* neighborhood partition function (Appendix H). The active exponents, which here depend through η_{1L} on both the flux J and the system's state, effectively behave as feedback agents—or "thermodynamic demons"—and exploit the information they have about the system to drive it perpetually out of equilibrium. In the next section we discuss a different mechanism sustaining a nonequilibrium steady state with a constant flux.

C. Active directed and diffusive motion

Active self-propelling particles constitute another class of nonequilibrium systems widely studied with the methods of statistical mechanics [113]. Here, we discuss two cases in which active particles move in a diffusive or a directed manner on a periodic lattice.

Each site of the whole lattice filled with self-propelling particles can be regarded as a subsystem. In the ensemble of such subsystems, the propensity of the particles to undergo directed active motion [114,115] can be described by a fraction $\psi_+ > 1/3$ of their total count N, which in a time step dt always jumps in the same direction from one site ℓ to the other $\ell+1$. This mechanism may describe a limited amount of "fuel" $N(\psi_+ - 1/3)$ available to power the directed motion [116] and thus bias the expected fraction of $1/3$ molecules moving in the chosen direction.

When $N, L \to \infty$, we expect to observe a total *cumulative* current in the whole system $J_{\mathrm{DM}} = \psi_+ N$. Therefore, instead of the constraint Eq. (34) we use

$$P_{\mathrm{DM}} = J_{\mathrm{DM}} - \sum_{\ell ji} n(\ell+1, j|\ell i) = 0. \tag{38}$$

Of course the direction of motion can be reversed if necessary.

By a similar token, active or enhanced diffusion [117,118] can be implemented by requiring a certain fraction of particles to jump to either side of the source site ℓ, rendering a cumulative displacement J_{AD}:

$$P_{\mathrm{AD}} = J_{\mathrm{AD}} - \sum_{\ell ji} (n(\ell-1, j|\ell i) + n(\ell+1, j|\ell i)). \tag{39}$$

By using the Lagrange multipliers η_{DM} and η_{AD} to the constraints P_{DM} and P_{AD}, respectively, we form the objective functions

$$f_{\mathrm{DM}} = f_0(\boldsymbol{s}_{dt}) + \eta_{\mathrm{DM}} P_{\mathrm{DM}}(\boldsymbol{s}_{dt}), \tag{40}$$

$$f_{\mathrm{AD}} = f_0(\boldsymbol{s}_{dt}) + \eta_{\mathrm{AD}} P_{\mathrm{AD}}(\boldsymbol{s}_{dt}). \tag{41}$$

By extremizing Eqs. (40) and (39) we obtain the most likely paths

$$n_{\mathrm{DM}}(mj|li) = g_j e^{-\beta\epsilon_j} \frac{n_i}{\zeta_\phi(\ell)} \exp(\hat{\phi}_{m\ell}), \tag{42}$$

$$n_{\mathrm{AD}}(mj|li) = g_j e^{-\beta\epsilon_j} \frac{n_i}{\zeta_\phi(\ell)} \exp(\tilde{\phi}_{m\ell}), \tag{43}$$

which are expressed here by using active exponents

$$\hat{\phi}_{m\ell} = \begin{cases} -\eta_{\mathrm{DM}} \text{ if } m = \ell+1, \\ 0 \text{ otherwise}, \end{cases} \tag{44}$$

$$\tilde{\phi}_{m\ell} = \begin{cases} -\eta_{\mathrm{AD}} \text{ if } m \neq \ell, \\ 0 \text{ otherwise}, \end{cases} \tag{45}$$

cf. Appendixes H and I. We omit the derivation of the steady states in the active systems considered here, as it repeats the steps covered earlier in a straightforward manner.

In a system with a homogeneous structure of energy levels, all sites must be macroscopically equivalent. Therefore, due to symmetry considerations, the nonequilibrium conditions do not generate a gradient of particles in the steady state, even in the presence of a flux J_{DM}. Unlike the case of gradient-driven flow discussed in the previous section, here the active exponents (44) also contain a symmetric part—called *frenetic* in Ref. [26]—i.e., $\hat{\phi}_{\ell,\ell+1} + \hat{\phi}_{\ell+1,\ell} \not\equiv 0$ and $\tilde{\phi}_{\ell,\ell+1} + \tilde{\phi}_{\ell+1,\ell} \not\equiv 0$. This symmetric part gives rise to *active* fluctuations [96, Supplemental Material Sec. 2], as well as to the notions of effective temperature and force-dependent transport coefficients[4] (Appendix I).

D. Norton and Thévenin ensembles

Section III B describes a *microcanonical Norton ensemble* with a fixed current at the boundaries—a method sometimes invoked in nonequilibrium atomistic simulations; see Refs. [119–121] and Ref. [122, Sec. 6.6]. There exists a complementary approach, Thévenin ensemble [122, Sec. 6.6], which leverages the concept of ensemble equivalence to fix, instead of the current J, its conjugate potential [123,124]. Such ideas have already been put into practice, e.g., to model heat flow [125].

In Sec. III B the microcanonical principle of maximum caliber identifies the Lagrange multiplier η—called *current affinity* in the following—as the conjugate variable of the boundary flux J that does not correspond precisely to the phenomenological quantities found in the literature [123–125]. By using our approach, we can analyze how and when the duality between a current and its affinity allow the equivalence of Norton and Thévenin ensembles (Sec. IV).

The equivalence of Norton and Thévenin ensembles has already been investigated by applying the methods of

[4]Here synonymous to nonlinear constitutive relations.

large-deviation theory to *time-averaged* variables [16,121]. Specifically, if the probability of such a variable $A_{\mathcal{T}}$ can be approximated by a rate function $I(A_{\mathcal{T}})$, which is convex at a point $\hat{A}$, as $p(A_{\mathcal{T}}) \asymp e^{-\mathcal{T} I(A_{\mathcal{T}})}$ in the limit of $\mathcal{T} \to \infty$, then the ensemble conditioned on $A_{\mathcal{T}} = \hat{A}$ is equivalent to an ensemble constrained by a thermodynamic conjugate to $A_{\mathcal{T}}$. In contradistinction, we focus here on the *instantaneous* quantities ($\mathcal{T} = dt \to 0$), which are more relevant to many modeling problems [126–128]. Nonetheless, the large-deviation principle is still applicable to some of these quantities by using the parameter of system size L instead of time $\mathcal{T}$.

As a counter example of Norton-Thévenin equivalence we also consider below the directed motion from Sec. III C, since both the directed motion and active diffusion can be classified as Norton ensembles with the cumulative flux J_{DM} and displacement J_{AD} as the generalized currents. However, as we discuss further, a fixed affinity η_{DM} does not generate the same statistics of the macroscopic flow as the constrained current J_{DM} in this context.

Indeed, the current affinity $\eta < 0$, which is conjugate to the boundary flux J, increases the fraction of particles that jump from the site L to 1, cf. Eq. (H7) with $\phi_{L1} = -\eta$. Likewise, it decreases the fraction of transitions in the reverse direction. Given that the steady state is on average characterized by a constant number of particles $\bar{\nu}_\ell$ with a global gradient $\bar{\nu}_{\ell+1} - \bar{\nu}_\ell \neq 0$, the biases of transition probabilities p_{1L} and p_{L1} sustain the constant flow $J = p_{1L}\bar{\nu}_L - p_{L1}\bar{\nu}_1$. Therefore, in the steady state the current affinity, which in the Norton ensemble is a thermodynamic observable, should also attain its stationary value $\langle\eta\rangle$ in correspondence to $\bar{\nu}_1$ and $\bar{\nu}_L$.

If instead of the current J_{1L} we fix the current affinity at the above value $\langle\eta\rangle < 0$, then we can generate a microcanonical Thévenin ensemble, whose steady state must also be characterized by a gradient, as well as by a fluctuating flux of the mean value $\langle J_{1L}\rangle$ that compensates for the bias in p_{1L} and p_{L1} by $p_{1L}(\eta)\bar{\nu}_L - p_{L1}(\eta)\bar{\nu}_1 - \langle J_1\rangle = 0$. Here all the parameter values must be equal to those of the steady-state Norton ensemble. However, in the bulk of these two systems, dynamics is driven by the same transition probabilities. In absence of long-range correlations, an example of which we discuss shortly, the effect of fluctuations in the current affinity η about its mean $\langle\eta\rangle$ or in the current J_{1L} should be negligible away from the boundaries. Therefore in the steady state both ensembles should be characterized by the same average values of thermodynamic variables, when measured in the bulk of the system. Hence the Norton and Thévenin pictures are equivalent in this scenario.

However the directed motion formulated in Sec. III C creates long-range correlations across the whole system and thus destroys the equivalence of Norton and Thévenin ensembles. In particular, assuming the homogeneous structure of energy levels, the variance of the total flux $J_+ = \sum_\ell n_{(\ell+1)\ell} = J_{\mathrm{DM}}$, being the fixed quantity, must vanish:

$$\mathrm{Var}(J_+) = L\mathrm{Var}(n_{(\ell+1)\ell}) + \sum_{\ell m} \mathrm{Cov}(n_{(\ell+1)\ell}, n_{(m+1)m}) = 0, \tag{46}$$

which implies that covariances $\mathrm{Cov}(n_{(\ell+1)\ell}, n_{(m+1)m})$ between the numbers of transferred particles $n_{(\ell+1)\ell}$ and $n_{(m+1)m}$ all add up to a negative value to cancel the term $L\mathrm{Var}(n_{(\ell+1)\ell}) > 0$ in Eq. (46).

In other words, the currents between *all* sites of the lattice in the directed motion are negatively correlated: more particles moving to the right from one site imply fewer particles moving to the right from another site, and vice versa. This anticorrelation would be totally lost if we fix η_{DM} instead of the cumulative current J_{DM}. In fact, this latter scenario would generate a steady state with the fraction of transitions to the right fixed *independently* at each site. Depending on the system, such a constraint may be of interest, e.g., in the limit where the fuel powering the directed motion is available in abundance [116] or scales as $L \to \infty$ in the limit of a large system.

In fact, the last scenario, in which scaling with system size L is present, can be related to the large-deviation results of Refs. [16,121] if we introduce the space-averaged flux $J_L = J_{\mathrm{DM}}/L$. Indeed, it is straightforward to verify that Eq. (13) entails an equilibrium state, in which J_L satisfies the large-deviation principle with a convex rate function. Consistently with Refs. [16,121], the Thévenin ensemble with an affinity η_L conjugate to J_L is equivalent to the Norton ensemble with the space-averaged flux $J_L = \tilde{J}_L$ enforced by a Lagrange multiplier η_L. However, these two ensembles are both distinct from the directed motion, or the boundary-driven ensemble of Sec. III B.

An important consequence of the anticorrelation Eq. (46) is suppression of current fluctuations demonstrated numerically in the following section. By losing this long-range correlation effect, a fixed affinity $\eta_{\mathrm{DM}} = -\hat{\phi}$ actually amplifies current fluctuations in the system by a factor of $3[2 + \exp(-\hat{\phi}/2)]^{-1} > 1$ (Appendix I).

IV. NUMERICAL EXAMPLES

To illustrate the theoretical results of Sec. III, we report below numerical simulations of a toy model on a small lattice of size $L = 3$ [129]. Specifically, we consider the Boltzmann gas with a homogeneous structure of energy levels characterized by the same local partition function $z(\ell \in \{1, 2, 3\}) = z$. Furthermore, by summing out all the energy levels through the coarse-graining procedure described in Appendix G, we reduce the Markov chain (28) to

$$\boldsymbol{\nu}(t + dt) = \boldsymbol{p} \cdot \boldsymbol{\nu}(t), \tag{47}$$

in which $\boldsymbol{\nu} = (\nu_1, \nu_2, \nu_3)$ is the vector of occupation numbers at each lattice site and $\boldsymbol{p}$ is the transition matrix. We analyze five distinct steady states to discuss several different features of nonequilibrium ensembles:

(1) As a baseline of comparison we consider equilibrium (Sec. III A), in which all elements of the transition matrix $p_{\ell m} \equiv z/\zeta = 1/3$ are equal.

(2) Diffusion driven by a constant boundary flux J (Sec. III B) is the paradigmatic example of a system with a spatial gradient and flow of matter driven by a matrix

$$\boldsymbol{p}(\eta) = \begin{pmatrix} (2+e^{\eta})^{-1} & 1/3 & (2e^{\eta}+1)^{-1} \\ (2+e^{\eta})^{-1} & 1/3 & (2+e^{-\eta})^{-1} \\ (2e^{-\eta}+1)^{-1} & 1/3 & (2+e^{-\eta})^{-1} \end{pmatrix}, \tag{48}$$

parameterized by the current affinity η.

(3) Diffusion driven by a constant current affinity $\eta \equiv$ const, which fixes $\boldsymbol{p}$ through Eq. (48), illustrates the concept of equivalence between nonequilibrium ensembles.

(4) Active self propulsion with a fixed cumulative current $J_{\rm DM}$ sustained by a matrix $\boldsymbol{p}(\eta_{\rm DM})$ with elements

$$p_{ij} = \begin{cases} (1+2e^{\eta_{\rm DM}})^{-1} \text{ if } i = j+1, \\ (2+e^{-\eta_{\rm DM}})^{-1} \text{ otherwise,} \end{cases} \tag{49}$$

parametrized by the current affinity $\eta_{\rm DM}$. This case provides an example of matter flow in absence of a spatial gradient and with suppressed level of current fluctuations.

(5) Active diffusion with a fixed cumulative displacement $J_{\rm AD}$ generated by a matrix $\boldsymbol{p}(\eta_{\rm AD})$ with elements

$$p_{ij} = \begin{cases} (2+e^{\eta_{\rm DM}})^{-1} \text{ if } i \neq j, \\ (1+2e^{-\eta_{\rm DM}})^{-1} \text{ otherwise,} \end{cases} \tag{50}$$

which entails neither spatial gradient nor macroscopic flow of matter, but amplifies microscopic fluctuations of the latter.

To perform *stochastic* simulations of steady states 2, 4, and 5, we designed an algorithm (Appendix J), which ensures the apposite constraints in each realization of the process $\boldsymbol{\nu}(t)$ [129]. The Lagrange multipliers η, $\eta_{\rm DM}$, $\eta_{\rm AD}$ become observable random variates. Our algorithm is also applicable to lattices of sizes $L > 3$, but for conspicuity, we present the results of the minimal model with $L = 3$—the smallest size that, under periodic boundary conditions, allows a division into subsystems S_0 and $\bar{S}_0$ as described in Sec. III B.

In our simulations we compute averages of the occupation numbers $\langle \boldsymbol{\nu} \rangle$, the gradient $\langle \text{grad}\, \nu \rangle = \langle \nu_3 - \nu_1 \rangle / 2$, and the macroscopic flux $\langle J_2 \rangle = \langle n_{21} - n_{12} \rangle$ through the lattice site $\ell = 2$ together with its variance $\text{Var}(J_2)$ over a single long trajectory. Here $n_{m\ell}$ is the count of particles transferred from the ℓth site to the mth in a single step. In addition, in case 2 we measure the current affinity $\langle \eta \rangle$, whose average value is then used to simulate case 3.

Because any transitions of particles between the three lattice sites are allowed, all simulations converge to steady states rather rapidly [Fig. 3(a)]. For the equilibrium case 1 ($\langle J_2 \rangle \equiv 0$), we observe a flat uniform distribution $\nu = N/L$ ($\langle \text{grad}\, \nu \rangle \equiv 0$). However, this same profile corresponds to the nonequilibrium steady states of directed motion 4 and active diffusion 5 as well. In contrast, the constraint of a constant boundary flux generates a steady state with a gradient within the system, as we predict (Sec. III B). By Kirchhoff's law the averaged flux in the central region of the system satisfies the equality $\langle J_2 \rangle = J$. We also verify the equivalence of Norton and Thévenin nonequilibrium ensembles 2 and 3, respectively. The constant current affinity η, set in case 3 at the average value observed in the Norton ensemble 2, generates within the statistical uncertainties the current $\langle J_2 \rangle = J$ and the gradient $\langle \text{grad}\, \nu \rangle$ of the same magnitude and direction.

Our simulations clearly reveal that the absence or presence of the current in the system does not completely determine the statistical signatures of the steady-state ensemble. In cases 1–3 currents of vanishing or nonzero magnitude are characterized by the same amplitude of fluctuations [Fig. 3(b)], but different distributions of particles. The directed motion of particles, case 4, generates the same macroscopic flow $\langle J_2 \rangle$ as in cases 2 and 3, but the amplitude of its fluctuations is even lower than in equilibrium. Finally, a uniform profile of particles is observed in equilibrium 1, steady states 4 and 5, but the mean value and variance of the flow J_2 differ across all these three cases.

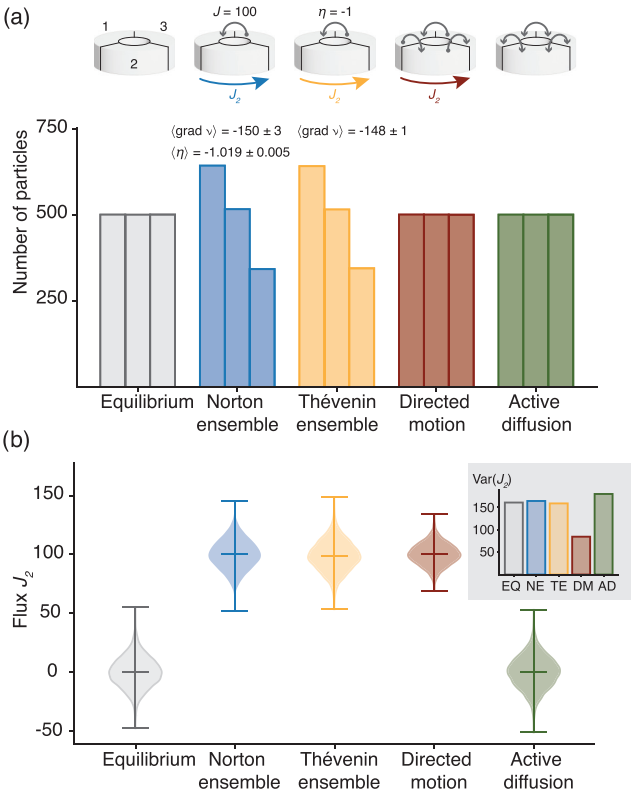

FIG. 3. Diffusion of $N = 1500$ particles on a periodic lattice of size $L = 3$ under various conditions: (1) Equilibrium conditions (EQ); (2) Norton ensemble (NE) with a fixed boundary flux $J = 100$; (3) Thévenin ensemble (TE) with a fixed current affinity $\eta = -1$; (4) Directed motion (DM) with a fixed cumulative current $J_{\rm DM} = 700$; (5) Active diffusion (AD) with a fixed cumulative displacement $J_{\rm AD} = 1100$. (a) Steady-state distributions of particles over lattice sites. Top icons summarize the simulation conditions. (b) Distributions of the particles' current J_2 through the site 2. The inset compares the variances $\text{Var}(J_2)$ between different ensembles. Stochastic simulations of the Markov chain Eq. (47) are performed for 10 100 steps starting from a uniform distribution $\nu_i = N/L$ by applying a Gillespie-like algorithm (Appendix J). Measurements are taken over the last 10 000 simulation steps undersampled to 1000 to ensure relaxation of the transient correlations. Standard errors correspond to five standard deviations of the mean.

The variance $\text{Var}(J_2)$ differs between cases 1–3 and 4–5. In the context of case 5 the active exponents contain a nonvanishing symmetric—frenetic—part $\phi_{m\ell} + \phi_{\ell m} \not\equiv 0$, which affects the amplitude of fluctuations in the system (Appendix I). When this part is positive or negative, the level of stochastic noise in the system can be amplified or suppressed, respectively. In the case 4, however, the cause of suppressed noise is the anitcorrelation constraint Eq. (46) that reduces the fluctuations of the currents n_{12}, n_{23}, and n_{31}.

V. DISCUSSION

Sections III and IV outline a general theory of microcanonical caliber for a large class of systems. While further details of this theory and its specific applications require separate dedicated studies, we highlight areas in which our framework provides new theoretical insights.

Beyond detailed-balance relations. To account for spontaneous fluctuations, which play an important role at meso- and microscopic scales, stochastic models of small thermodynamic systems are usually designed to observe the detailed-balance condition in the limit of vanishing nonequilibrium forces [17,26,27,39,130]. For example, in the context of master equations and discrete state spaces it is typically expressed as a ratio of the forward transition rates k_{ji} from a state $\boldsymbol{s}_i$ to $\boldsymbol{s}_j$ and its reverse k_{ji} [131, Chapter 3]:

$$\frac{k_{ji}}{k_{ij}} = e^{-\beta(F(\boldsymbol{s}_j)-F(\boldsymbol{s}_i)+\Delta W)}, \tag{51}$$

where $F(\boldsymbol{s})$ is a free energy of a state $\boldsymbol{s}$ and ΔW is the work done on the system by nonequilibrium forces. Indeed, the above equation is at the foundations of the stochastic-thermodynamics formalism [26,131].

How general is Eq. (51) in nonequilibrium systems? The condition of local detailed balance can be related to the first principles of classical microscopic dynamics [27,28,85,86], although generalizations due to complex interactions exist, e.g., in Fermi-Dirac systems [110,111] (Sec. II B). This latter relation (22), as well as further generalizations (12), (29), (21), (37), and (G3), were routinely deduced here from the single principle of maximum caliber.

Indeed the microcanonical principle of maximum caliber provides a systematic means to derive and study the relation (51) with its generalization by *direct calculations*. In special cases Eq. (51) may emerge under coarse graining like Eq. (G3), in the mean-field approximation, or by taking the limit of Eq. (29) with $g_i(\ell) = O(g_j(m))$ and $\zeta(\ell) = O(\zeta(m))$.

Fluctuations in nonequilibrium systems. As shown in Secs. III B and III C, distinct nonequilibrium states can be generated by applying active exponents ϕ_{ij}, which break the detailed balance. Our framework relates the statistics of fluctuating variables in such systems to constraints imposed on the microscopic dynamics, revealing how different driving mechanisms produce distinct statistical signatures, as discussed in Sec. IV. These mechanisms may entail generalized forms of the fluctuation-dissipation theorem involving effective temperature and force-dependent transport coefficients (Appendix I). Therefore the microcanonical principle of maximum caliber also provides means to analyze the effect of nonequilibrium forces on the spontaneous fluctuations in thermodynamic systems.

Space-dependent diffusion. External fields, such as chemical interactions at phase interfaces, sometimes cause two effects simultaneously: an effective thermodynamic potential $U(x)$ and a space-dependent diffusion coefficient $D(x)$ that appear in the Smoluchowski equation (G4) as independent parameters [132,133]. In the simplified model of Sec. III A, such external fields could be described by a spatially inhomogeneous structure of energy levels summarized by neighborhood and local partition functions, $\zeta(\ell)$ and $z(\ell)$, which simultaneously generate a space-dependent diffusion coefficient $D(x)$ and an effective potential $U(x)$ derived in Appendix G. Thereby the microcanonical principle of maximum caliber reduces the two parameters of the Smoluchowski equation to a single origin and unifies phenomena of inhomogenous energetic and transport properties in thermodynamic systems.

Previously Ghosh *et al.* [66] derived the diffusion equation without the potential term from the principle of maximum caliber, recovering the same formula for the transport coefficient $D \propto \kappa dt$ (where κdt is the escape probability, cf. Appendix G) as in the classical treatment of random walks [134, Chapter I]. The microcanonical approach offers further insights into the statistical origin of the escape probability, which in the traditional theory appears as an opaque phenomenological parameter. Its emergence from the microscopic energy structure and dependence on the temperature are summarized by the partition functions $\kappa dt \propto z(\beta)/\zeta(\beta)$.

Inhomogeneities in the system may also emerge due to a complex graph-theoretical structure of allowed state transitions [135–137]. Their effects may generate phenomena of nontrivial localization and, in combination with space-dependent transport properties, kinetic arrest and traps [14,138].

General transport processes. Unlike the original works of Filyukov and Karpov [57], this paper develops the microcaliber framework for systems involving transport of matter, which is perhaps the simplest nonequilibrium phenomenon. Other processes frequently considered in the theoretical research on the maximum-caliber principle are heat and momentum transport, e.g., Refs. [28,57,58,61,73,85,86].

From the microcanonical perspective explored here, the theory of heat transport is more complicated, because to specify a system's path, in addition to the number of particles transferred between the energy levels, e.g., n_{ji} in Sec. II A, one must also specify how the energy is being redistributed. Given that the energies of the source and target levels are in general not equal $\Delta\epsilon = \epsilon_j - \epsilon_i \neq 0$, additional constraints on the microscopic dynamics are necessary. For example, a transfer of particles n_{ji} must be accompanied by another transfer $n_{m\ell}$ to compensate $\epsilon_m - \epsilon_\ell = -\Delta\epsilon$. The Lagrange multiplier β maintains the global energy balance ensuring that all such changes everywhere in the systems add up to zero. Thereby the specific information about how much energy a particular transition $n_{m\ell}$ donates to or receives from another transition n_{ji} is lost. In spatially extended systems, considerations of the macroscopic continuity equation for the energy, similar to Eq. (24) for the number of particles, also come into focus, as the donor and acceptor transitions should reside within some neighborhood of each other.

The linear momentum is an example of another thermodynamic variable that can be introduced into the framework and accounted for separately to model related transport processes. At the level of microscopic dynamics additional constraints are required as well.

The above details, which are bypassed in the traditional approach to the maximum-caliber principle using the concept of thermodynamic reservoirs, should be explicitly developed at the level of microcanonical theory—a viable program that can now be pursued.

First principles of microscopic dynamics. Ensemble theory is a cornerstone of statistical mechanics [49,83,139,140], rooted in the Hamiltonian deterministic dynamics of equilibrium systems, and more recently extended also to non-hamiltonian dynamics of dissipative systems [43,141–143]. This theory provides the foundations of molecular-dynamics methods and guides the development of algorithms for nonequilibrium simulations [83,122,144]. In fact, the theory of ensembles was developed by Boltzmann with the intent of describing the thermodynamic behavior of macroscopic systems, in the limit in which microscopic fluctuations are not observable. However, it turns out to be particularly useful in present-day science and technology dealing with small systems, in regimes where fluctuations cannot be neglected.

The mechanism of nonequilibrium driving introduced in Sec. III B resembles the approaches developed in Refs. [120,145,146] for atomistic modeling. Therefore, a connection between the microcaliber theory and dynamical-systems formalism might be quite fruitful.

Our framework relies on the identification of key constraints for microscopic dynamics, which capture the essential properties of the physical systems being modeled. Due to the deterministic nature of classical physics, given coordinates $\boldsymbol{q}(t)$ and velocities $\dot{\boldsymbol{q}}(t)$ of the particles, there is in general a single dynamical constraint corresponding to Newton's second law,

$$\begin{aligned}\boldsymbol{q}(t+dt) &= \boldsymbol{q}(t) + dt\dot{\boldsymbol{q}},\\ \dot{\boldsymbol{q}}(t+dt) &= \dot{\boldsymbol{q}}(t) + \frac{dt}{m}\boldsymbol{F}(\boldsymbol{q}),\end{aligned} \tag{52}$$

where we assume conservative forces $\boldsymbol{F}(\boldsymbol{q}) = \partial H/\partial \boldsymbol{q}$ within the microcanonical approach, and equal masses of particles m.

Once the initial state $\boldsymbol{s}(0) = (\boldsymbol{q}(0), \dot{\boldsymbol{q}}(0))$ is specified, only one realization of the system's path $\boldsymbol{s}_t = (\boldsymbol{q}(t), \dot{\boldsymbol{q}}(t))$ is possible, which can be formally written using the multidimensional δ function:

$$\begin{aligned}\Omega_{\mathcal{T}}\big(\boldsymbol{s}(0)\big) \propto \int_{\sigma\times\mathcal{T}} \mathcal{D}\boldsymbol{s}_t \int_{\sigma} \boldsymbol{ds}\, \boldsymbol{\delta}\big(\boldsymbol{s}-\boldsymbol{s}(0)\big)\\ \times \boldsymbol{\delta}\bigg(\int_{\mathcal{T}} dt\, \frac{\delta\mathcal{L}}{\delta \boldsymbol{q}(t)}\bigg),\end{aligned} \tag{53}$$

where $\mathcal{L}$ is the system's *Lagrangian* concisely summarizing Eq. (52). If the system is subject to periodic boundary conditions, then the Lagrangian formalism can incorporate additional constraints and forces, such as those generating nonequilibrium driving in Sec. III. For example, one can add a constant force on all particles together with a constraint of conserved energy to produce active flow as in Sec. III C.

In the context of dynamical systems, the uncertainty addressed by statistical methods may arise due to unknown initial-value conditions $\boldsymbol{s}(0)$, which can be characterized by a probability distribution $p_\sigma(\boldsymbol{s}(0))$. This probability can replace the first δ function in Eq. (53)—formally by performing a convolution $p_\sigma * \Omega_{\mathcal{T}}(s(0))$.

Conclusion. The microcanonical approach brings various physical insights, which can be applied well beyond the scope of this work, including information-theoretic tools developed for the maximum-caliber principle. These insights can also be combined with the concepts of canonical and other ensembles through the usual thermodynamic techniques [83,84]. In fact, Sec. IV explores one such example—the equivalence of the Norton and Thévenin ensembles. Finally the principle of maximum caliber may serve as a platform for unifying different theoretical approaches in statistical mechanics, such as random walks and dynamical systems.

ACKNOWLEDGMENTS

R.B., J.E., and A.E. acknowledge funding from the EMBL. L.R. is members of the Gruppo Nazionale per la Fisica Matematica (GNFM) of Istituto Nazionale di Alta Matematica. L.R. acknowledges funding from Theory@EMBL Transversal Theme and is grateful for the work hospitality received at EMBL during a sabbatical visit. L.R. also acknowledges support from the Italian Ministry of University and Research (MUR) through the Grant No. PRIN2022-PNRR Project (No. P2022Z7ZAJ) "A Unitary Mathematical Framework for Modelling Muscular Dystrophies" (CUP E53D23018070001) funded by the European Union - Next Generation EU. The authors are grateful to Laeschkir Würthner, Patrick Jentsch, Pamela Guruciaga, Ian Estabrook, Tim Dullweber, and Johannes Jung for stimulating discussions.

DATA AVAILABILITY

The data that support the findings of this article are openly available [129].

APPENDIX A: MAXIMUM ENTROPY AND MAXIMIUM CALIBER

Equation (2) defining the system caliber owes its inception to a peculiar mathematical property it shares with (Shannon-) Gibbs entropy Eq. (1), when regarded as a functional of probability distribution functions [32,63,65,79,147,148]. If we impose constraints on some macroscopic variables $\langle c_{i=0,1,2,\dots}(\boldsymbol{s})\rangle = \bar{c}_i$ with known values $\bar{c}_i$, including the normalization condition $\int_{\boldsymbol{\sigma}} \boldsymbol{ds}\, p_\sigma(\boldsymbol{s}) = 1$ as $c_0(\boldsymbol{s}) \equiv 1$, and maximize S_σ with respect to $p_\sigma(\boldsymbol{s})$, using the Lagrange multipliers $\lambda_{i=0,1,\dots}$, then we obtain (see below)

$$p_\sigma(\boldsymbol{s}) \propto \exp\left(-\sum_{i=0,1,2,\dots} \lambda_i c_i(\boldsymbol{s})\right). \tag{A1}$$

For example, if we choose $c_1(\boldsymbol{s}) = E(\boldsymbol{s})$ to be the system's energy, then Eq. (A1) yields the canonical distribution $p_\sigma(\boldsymbol{s}) = Z^{-1}\exp[-E(\boldsymbol{s})/(k_B T)]$ with the partition function $Z = e^{1+\lambda_0}$, and temperature $T = (k_B\lambda_1)^{-1}$.

To maximize the Shannon-Gibbs entropy (1) with respect to the distribution $p_\sigma(\boldsymbol{s})$ subject to the constraints on $\langle c_{i=0,1,2}(\boldsymbol{s})\rangle = \bar{c}_i$, we form an objective functional including Lagrange multipliers λ_i:

$$\begin{aligned}F[p_\sigma(\boldsymbol{s})] &= S_\sigma + \sum_i \lambda_i\big(\bar{c}_i - \langle c_i(\boldsymbol{s})\rangle\big)\\ &= -\int_{\sigma} ds\, p_\sigma(\boldsymbol{s})\bigg[\ln p_\sigma(\boldsymbol{s}) + \sum_i \lambda_i c_i(\boldsymbol{s})\bigg] + \sum_i \lambda_i \bar{c}_i.\end{aligned} \tag{A2}$$

The variation of the objective function yields

$$\frac{\delta F}{\delta p_\sigma(\boldsymbol{s})} = -\left(\ln p_\sigma(\boldsymbol{s}) + 1 + \sum_i \lambda_i c_i(\boldsymbol{s})\right).$$

Imposing the condition of extremum $\delta F/\delta p_\sigma(\boldsymbol{s}) = 0$, we obtain

$$p_\sigma(\boldsymbol{s}) = e^{-1-\lambda_i \sum_i c_i(\boldsymbol{s})} = Z_\sigma^{-1} e^{-\sum_{i>0}\lambda_i c_i(\boldsymbol{s})}, \tag{A3}$$

in which we expanded the constraint $c_0(\boldsymbol{s}) \equiv 1$ of the normalized probability density $\bar{c}_0 = 1$ and introduced the partition function $Z_\sigma = \exp(1+\lambda_0)$.

By a similar token, $S_\mathcal{T}[p(\boldsymbol{s}_t)]$, regarded as a higher-order functional, can be extremized with respect to $p_\mathcal{T}(\boldsymbol{s}_t)$—the process that constitutes the *principle* of maximum caliber. Constraints imposed on macroscopic variables $\bar{C}_{i=0,1,2} = \langle C_i(\boldsymbol{s}_t)\rangle$ with the Lagrange multipliers $\lambda_{i=0,1,2}$, also including the condition of normalized probabilities, yield [38,73,79]

$$p_\mathcal{T}(\boldsymbol{s}_t) \propto \exp\left(-\sum_{i=0,1,2,\ldots} \lambda_i C_i(\boldsymbol{s}_t)\right). \tag{A4}$$

A variable $C_1(\boldsymbol{s}_t) = Q(\boldsymbol{s}_t)$ often proposed to describe statistics of nonequilibrium steady states [57,73], is the time-averaged heat transfer

$$Q(\boldsymbol{s}_t) = \int_\mathcal{T} \frac{dt}{\mathcal{T}}\, q(\boldsymbol{s}_t),$$

in which $q(\boldsymbol{s}_t)$ is the instantaneous value of the heat current.

APPENDIX B: BOLTZMANN DISTRIBUTION

Here we summarize the modern formulation of the microcanonical distribution for the simplified model of Boltzmann gas consisting of indistinguishable particles (Sec. II A), e.g., Ref. [95, Chapters 12 and 13]. A distribution of particles over energy levels $i = 1, 2, \ldots, M$ is specified by occupation numbers $\{n_i\}_{i=1}^M$ with the count of realizations W given by the Maxwell-Boltzmann statistics

$$W \approx \prod_{i=1}^M \frac{g_i^{n_i}}{n_i!}.$$

Assuming that all realizations are equivalent, we extremize the objective function

$$f_W = \ln W + \alpha(N - \sum_i n_i) + \beta(E - \sum_i \epsilon_i n_i),$$

where the Lagrange multipliers α and β incorporate the constraints on the total number of particles N and their energy E. By extremizing f_W, we get

$$n_i = g_i e^{-\alpha-\beta\epsilon_i}. \tag{B1}$$

The Lagrange multiplier α can be evaluated in this model explicitly from the constraint

$$N = \sum n_i = e^{-\alpha} Z_{\mathrm{MB}},$$

which yields $\alpha = -\ln(N/Z_\mathrm{B})$. Now we identify the Boltzmann entropy with

$$S_\mathrm{B} = k_\mathrm{B} \ln W = k_\mathrm{B} N + k_\mathrm{B}\beta E + k_\mathrm{B}\alpha N,$$

which yields the Euler equation when multiplied by T:

$$TS_\mathrm{B} = Nk_\mathrm{B}T + TE - \mu_{\mathrm{MB}} N,$$

with the chemical potential $\mu_{\mathrm{MB}} = -k_\mathrm{B}T\alpha$. By replacing the Lagrange multiplier $\alpha = -\beta\mu_{\mathrm{MB}}$ in Eq. (B1), we get Eq. (14).

Note that to obtain the Boltzmann probability distribution we need to normalize Eq. (14), which amounts to division by N and yields the fraction of particles residing in the energy level ϵ_i in equilibrium:

$$p_i = \frac{g_i}{N} e^{\beta(\mu_{\mathrm{MB}}-\epsilon_i)} = \frac{g_i}{Z_{\mathrm{MB}}} e^{-\beta\epsilon_i}.$$

APPENDIX C: EULER-LAGRANGE EQUATIONS FOR PATH FUNCTIONALS

By maximizing the constrained microcanonical caliber Eq. (7) over trajectories of infinitesimal duration dt, in Sec. II A we obtain the system's dynamics, which in the continuum limit $dt \to 0$ refers to instantaneous—*local in time*—quantities and their rates of change. In this Appendix we show constructively how this formalism gives rise to an entropy functional of the system's path over a finite interval $\mathcal{T}$—nonlocal in time—as it appears in the traditional principle of maximum caliber.

By partitioning the interval $t \in (0, \mathcal{T}]$ into R equal subintervals, so that $\mathcal{T} = Rdt$, we define a time series of objective functions

$$f^r_{\mathrm{MB}} = \ln \Omega_{\mathrm{MB}}\left(\{n^r_{ji}\}\right) + \beta^r\left(E - \sum_{ij} \epsilon_j n^r_{ji}\right) + \sum_i \theta^r_i \left(n^{r-1}_i - \sum_j n^r_{ji}\right), \tag{C1}$$

with the superscript r abbreviating the time dependence $n^r_{ji} = n_{ji}(rdt)$, $\beta^r = \beta(rdt)$, etc. Then we form a discrete functional of a multistep path $\Gamma = \{n^r_{ji}\}_{r=1}^R$:

$$F_{\mathrm{MB}}(\Gamma) = \sum_r \left(f^r_{\mathrm{MB}} + \Delta f^r_{\mathrm{MB}}\right), \tag{C2}$$

where the term

$$\Delta f^r_{\mathrm{MB}} = \sum_j \chi^r_j \left(n^{r+1}_j - \sum_i n^r_{ji}\right) + \alpha^r\left(N - \sum_{ij} n^r_{ji}\right)$$

"glues" together the pieces n^r_{ji} of the whole trajectory Γ, by imposing the constraint on the total number of particles N (Appendix B), and the second constraint in Eq. (4) with the Lagrange multipliers α^r and χ^r_j, respectively. Note that $n^0_i = n_i(0)$ is fixed as the initial condition.

By construction the condition of extremum for F_{MB} reads

$$0 = \frac{\delta F_{\mathrm{MB}}}{\delta n^r_{ji}} = \frac{\partial f^r_{\mathrm{MB}}}{\partial n^r_{ji}} + \frac{\partial \Delta f^r_{\mathrm{MB}}}{\partial n^r_{ji}}, \tag{C3}$$

which represents a discretized Euler-Lagrange equation and yields a generalized version of Eq. (9),

$$n^r_{ji} = g_j e^{-\chi^r_j - \beta^r\epsilon_j - \theta^r_i - \alpha^r}. \tag{C4}$$

First we evaluate the multipliers χ_j^r from

$$e^{-\chi_j^r} = \frac{n_j^{r+1} e^{\beta^r \epsilon_j}}{g_j \sum_i e^{-\theta_i - \alpha^r}},$$

and therefore

$$n_{ji}^r = n_j^{r+1} \frac{e^{-\theta_i - \alpha^r}}{\sum_i e^{-\theta_i - \alpha^r}}. \tag{C5}$$

Note that in Eq. (C5) we do not cancel out α^r, while it is possible, to keep in evidence the "gauge" freedom of the constraints

$$n_i^{r-1} = \sum_j n_{ji}^r = \frac{N e^{-\theta_i^r - \alpha^r}}{\sum_i e^{-\theta_i^r - \alpha^r}}. \tag{C6}$$

Indeed, Eq. (C6) specifies θ_i^r up to an arbitrary additive constant α^r, which we choose so that

$$e^{-\theta_i^r - \alpha^r} = \frac{n_i^{r-1}}{Z_{\mathrm{MB}}(\beta^r)}. \tag{C7}$$

Because the total number of particles is conserved at all time steps r, recombining Eq. (C4) with Eq. (C7), we observe that

$$\begin{aligned} N &= \sum_{ij} n_{ji}^r = \sum_{ij} g_j e^{-\chi_j - \beta^r \epsilon_j} \frac{n_i^{r-1}}{Z_{\mathrm{MB}}^r} \\ &= \frac{N}{Z_{\mathrm{MB}}^r} \sum_j g_j e^{-\chi_j - \beta^r \epsilon_j} \end{aligned} \tag{C8}$$

entails

$$Z_{\mathrm{MB}}^r = \sum_j g_j e^{-\beta^r \epsilon_j} = \sum_j g_j e^{-\chi_j - \beta^r \epsilon_j}$$

for *any set* of χ_j^r in the chosen gauge α^r. Hence, we get

$$n_{ji}^r = g_j e^{-\beta^r \epsilon_j} \frac{n_i^{r-1}}{Z_{\mathrm{MB}}(\beta^r)}. \tag{C9}$$

Equation (C9), derived from the time-nonlocal functional F_{MB}, is therefore equivalent to Eq. (11) obtained by maximizing time time-local objective function $f_{\mathrm{MB}}(t)$ at any instance $t = rdt$ as in Sec. II A.

APPENDIX D: FROM MARKOV CHAINS TO MASTER EQUATION

The right hand-side of the Markov chain Eq. (13) can be expanded as

$$n_j(t + dt) = n_j(t) + dt\, \partial_t n_j(t) + O(dt^2),$$

from which we obtain

$$\begin{aligned} \partial_t n_j + O(dt) &= \frac{\sum_i p_{ji} n_i - n_j}{dt} \\ &= \sum_i \frac{p_{ji} n_i - p_{ij} n_j}{dt} = \sum_{i \neq j} \frac{p_{ji} n_i - p_{ij} n_j}{dt}, \end{aligned} \tag{D1}$$

where we use Eq. (4) for $n_j(t)$ and omit its explicit time-dependence for brevity. With Eq. (15), the limit $dt \to 0$ of the above equation yields a master equation of a Markov process $n_i(t)$:

$$\partial_t n_i(t) = \sum_{j \neq i} [k_{ij} n_j(t) - k_{ji} n_i(t)]. \tag{D2}$$

APPENDIX E: MICROCANONICAL CALIBER OF FERMI GAS

To derive Eq. (17) for a given set of elements n_{ji}, we focus on a single target level j, while traversing the source levels in the increasing order of the index $i = 1, 2, \ldots$ first. The number of ways to allocate n_{j1} of particles transferred from the level $i = 1$ is given by the Fermi-Dirac statistic [95, Chapter 13]:

$$\Omega_{j1} = \frac{g_j!}{(g_j - n_{j1})! n_{j1}!}.$$

After that, there remain

$$\Omega_{j2} = \frac{(g_j - n_{j1})!}{(g_j - n_{j1} - n_{j2})! n_{j2}!}$$

ways to allocate n_{j2} particles transferred from the level $i = 2$. By induction, choosing a particular sequence of the levels $i = 1, 2, \ldots, M$ we obtain

$$\begin{aligned} \Omega_j = &\frac{g_j!}{\cancel{(g_j - n_{j1})!} n_{j1}!} \times \frac{\cancel{(g_j - n_{j1})!}}{\cancel{(g_j - n_{j1} - n_{j2})!} n_{j2}!} \times \ldots \\ &\times \frac{\cancel{\left(g_j - \sum_{i<M} n_{ji}\right)!}}{\left(g_j - \sum_i n_{ji}\right)! n_{jM}!} = \frac{g_j!}{\left(g_j - \sum_i n_{ji}\right)! \prod_i n_{ji}!}. \end{aligned} \tag{E1}$$

Remarkably, in the final expression of Eq. (E1) the dummy index i is eliminated from the denominator by the summation operator in the first factor $(g_j - \sum_i n_{ji})!$, and by the product operator in the second factor $\prod_i n_{ji}$. As commutative operators they *do not depend* on the order of operands n_{ji} and, hence, neither on the sequence, in which we traverse the source levels.

Therefore the $M!$ possible permutations of the index i, which specify the traversal order of the source levels, are indistinguishable and yield the same number of realizations Ω_j. As each target level j contributes toward the total count $\Omega(\boldsymbol{s}_{dt})$ of the whole path's realizations independently, Eq. (17) follows from

$$\Omega(\boldsymbol{s}_{dt}) = \prod_j \Omega_j.$$

To maximize the caliber of a Fermi-Dirac gas we make use of the Stirling approximation

$$\begin{aligned} \ln \Omega_{\mathrm{FD}} \approx \sum_j \Bigg\{ &g_j \ln g_j - g_j \\ &- \left(g_j - \sum_i n_{ji}\right) \left[\ln \left(g_j - \sum_i n_{ji}\right) - 1 \right] \\ &- \sum_i (n_{ji} \ln n_{ji} - n_{ji}) \Bigg\} \end{aligned} \tag{E2}$$

to form the objective function

$$f_{\rm FD} = \ln \Omega_{\rm FD} + \beta\left(E - \sum_{ij}\epsilon_j n_{ji}\right) + \sum_i \theta_i\left(n_i - \sum_{ij} n_{ji}\right), \tag{E3}$$

with Lagrange multipliers β and θ_i. The extremum condition $\partial f_{\rm FD}/\partial n_{ji} = 0$ then yields

$$n_{ji} = (g_j - n'_j)e^{-\beta\epsilon_j - \theta_i}, \tag{E4}$$

with $n'_j = n_j(t + dt)$. By imposing the constraint Eq. (4) on $n_i(t) = \sum_j n_{ji}$, we evaluate

$$e^{-\theta_i} = \frac{n_i}{\sum_j (g_j - n'_j)e^{-\beta\epsilon_j}}. \tag{E5}$$

Equations (E4) and (E5) combined together produce Eq. (18).

APPENDIX F: SIMPLIFIED MODEL OF PAIRWISE INTERACTIONS

Simplified models of the classical statistical mechanics, like those considered in Sec. II, can also be generalized to analyze multibody interactions between particles and are not limited to hard-core repulsion. Here we discuss briefly how to introduce pairwise interaction into the Boltzmann model of ideal gas (Sec. II A). To this end we extend the structure of energy levels now numbered by two indices $a = 1, 2$ and $b = 1, 2, ..., M$, where $a = 1$ labels isolated particles and $a = 2$ represents a doublet of interacting particles.

The occupation numbers n_{1b} and n_{2b} may be regarded as specifying two distinct types of particles, with the conversion between the two characterized by a chemical reaction $2n_{1b} \leftrightarrow n_{2b}$. The conservation of matter and energy takes then the following form of macroscopic constraints

$$N = \sum_{ab} a n_{ab}, \qquad E = \sum_{ab} a\epsilon_{ab} n_{ab}, \tag{F1}$$

in which $2\epsilon_{2b}$ stands for the energy of a doublet, which is shared equally between the constituent particles. The transition $n_{a'b'|ab}$ from an energy level ϵ_{ab} to $\epsilon_{a'b'}$ now requires four indices. The constraint (4) then should be recast as

$$a n_{ab}(t) = \sum_{a'b'} a' n_{a'b'|ab}, \quad a' n_{a'b'}(t + dt) = \sum_{ab} a n_{a'b'|ab}.$$

To take into account clusters of three or more interacting particles, energy levels ϵ_{ab} with $a = ...3, 4, ...$ of triplets, quadruplets, etc., can be considered. Such a straightforward extension enables modeling of either pairwise-additive potentials, or more complex multibody interactions. This formalism resembles, in fact, the cluster expansion in the classical statistical mechanics; see Ref. [149] and Ref. [97, Sec. 5.2].

APPENDIX G: COARSE-GRAINING AND CONTINUUM LIMIT OF LATTICE MODELS

Here we derive a space-dependent diffusion equation for the system discussed in Sec. III A, to illustrate two formal procedures applicable to lattice models, namely, coarse graining and taking the continuum limit of the sites' length scale $dx \to 0$. In principle, the continuum limit can also be taken without coarse graining, leading to reaction-diffusion equation, for brevity and simplicity of our example we combine both.

Although lattice models by themselves constitute a kind of coarse graining in space, in some physical contexts the information about distribution of particles over energy levels of the system is not accessible. In the problem of particles' diffusion, for example, this information is usually not taken into account. Using the spatial discretization we eliminate the distinction between energy levels at the lattice sites, by summing Eq. (28) describing a discrete random walk, over the index j:

$$\nu(m, t + dt) = \sum_j n_j(m, t + dt) = z(m) \sum_{\ell=m-1}^{m+1} \frac{\nu(\ell, t)}{\zeta(\ell)}. \tag{G1}$$

Applying the relation

$$z(m) = \zeta(m) - z(m + 1) - z(m - 1)$$

to Eq. (G1), we get

$$\partial_t \nu(m, t) = -\kappa(m)\nu(m) + k_{m,m+1}\nu(m + 1) + k_{m,m-1}\nu(m - 1), \tag{G2}$$

with transition rates $k_{m\pm1,m} = z(m \pm 1)/(\zeta(m)dt)$ (Appendix D), and escape rate $\kappa(m) = k_{m+1,m} + k_{m-1,m}$. Note that the transition rates satisfy a generalized local detailed-balance relation

$$\frac{k_{m,\ell}}{k_{\ell,m}} = \frac{z(m)\zeta(m)}{z(\ell)\zeta(\ell)} = \frac{\zeta(m)}{\zeta(\ell)} e^{\mathcal{U}(m)-\mathcal{U}(\ell)}, \tag{G3}$$

in which we identify a *directing* function [133]

$$\mathcal{U}(\ell) = \ln z(\ell).$$

The directing function may emerge, for example, due to external fields, such as gravity.

Now, if we interpret lattice indices ℓ as spatial coordinates $x = \ell\, dx$, then the random walk Eq. (G3) can be analyzed by standard methods [134, Chapters I and II]. In particular, due to the spatial dependency of $\kappa(x)$ the continuous limit of this random walk yields a Smoluchowski equation [133] for the density $\rho(x) = \nu(x)/dx$:

$$\partial_t \rho(x) = \nabla \cdot [\beta D(x)\nabla U(x)\rho(x) + D(x)\nabla\rho(x)], \tag{G4}$$

with a space-dependent diffusion coefficient

$$\frac{\kappa(x)dx^2}{2} \underset{\substack{dx\to0\\dt\to0}}{\to} D(x),$$

and the effective potential

$$U(x) = k_{\rm B}T(\ln D(x) - 2\mathcal{U}(x)).$$

In the presence of nonequilbrium constraints, e.g., with a Lagrange multiplier $\eta \in \{\eta_{1L}, \eta_{\rm DM}, \eta_{\rm AD}\}$ (Secs. III B and III C), the coarse-grained Eq. (G1) takes a more general form:

$$\nu_\ell(t + dt) = \sum_m p_{\ell m}(\eta)\nu_m(t), \tag{G5}$$

in which we simplify the notation $\nu_\ell(t) = \nu(\ell, t)$ and introduce the transition probabilities

$$p_{\ell m}(\eta) = \frac{z(m) w_{\ell m}(\eta)}{\zeta_\eta(m)}, \tag{G6}$$

where the extended partition function $\zeta_\eta(m)$ and a weight $w_{\ell m}(\eta)$ may in general depend on the Lagrange multiplier η. For example, in the gradient-driven flow discussed in Sec. III B, such a dependence appears in p_{L1} and p_{1L} with

$$w_{1L} = e^{-\eta_{1L}}, \quad \zeta_\eta(L) = z_{L-1} + z_L + z_1 w_{1L}, \tag{G7}$$

$$w_{L1} = e^{\eta_{1L}}, \quad \zeta_\eta(1) = w_{L1} z_L + z_1 + z_2, \tag{G8}$$

cf. Sec. IV.

APPENDIX H: CONSTRAINT OF CONSTANT FLUX AT THE BOUNDARY

By imposing the extremum condition $\partial f_{1L}/\partial n(mj|\ell i)$ on the objective function (35) near the end points $m, \ell = \{1, L\}$, we get

$$n(1j|Li) = g_j(1) e^{-\beta\epsilon_j(1) - \theta_i(L) - \eta_{1L}}, \tag{H1}$$

$$n(Lj|1i) = g_j(L) e^{-\beta\epsilon_j(L) - \theta_i(1) + \eta_{1L}}, \tag{H2}$$

whereas all the other transitions satisfy

$$n(mj|\ell i) = g_j(m) e^{-\beta\epsilon_j(m) - \theta_i(\ell)}. \tag{H3}$$

By evaluating the constraints associated with $\theta_i(\ell \notin \{1, L\})$ we obtain Eq. (27). To evaluate $\theta_i(\ell \in \{1, L\})$ we apply Eq. (24):

$$\begin{aligned} n_i(1,t) &= \sum_j (n(Lj|1i) + n(1j|1i) + n(2j|1i)) \\ &= e^{-\theta_i(1)} (e^{\eta_{1L}} z(L) + z(1) + z(2)), \end{aligned} \tag{H4}$$

$$\begin{aligned} n_i(L,t) &= \sum_j (n(L-1, j|Li) + n(Lj|Li) + n(1j|Li)) \\ &= e^{-\theta_i(L)} (z(L-1) + z(L) + z(1) e^{-\eta_{1L}}). \end{aligned} \tag{H5}$$

By solving the two above equations for the Lagrange multipliers $\theta_i(\ell \in \{1, L\})$, from Eqs. (H1) and (H2) we obtain

$$n(1j|Li) = \frac{g_j(1)}{\zeta_{\eta_{1L}}(L)} e^{-\beta\epsilon_j(1) + \phi_{1L}} n_{Li} = p(1j|Li, J) n_i(L), \tag{H6}$$

$$n(Lj|1i) = \frac{g_j(L)}{\zeta_{\eta_{1L}}(1)} e^{-\beta\epsilon_j(L) + \phi_{L1}} n_{1i} = p(Lj|1i, J) n_j(L), \tag{H7}$$

in which we introduce active exponents [96] $\phi_{1L} = -\eta_{1L}$, $\phi_{L1} = \eta_{1L}$, and extended neighborhood partition functions

$$\zeta_\phi(1) = e^{\phi_{L1}} z(L) + z(1) + z(2), \tag{H8}$$

$$\zeta_\phi(L) = z(L-1) + z(L) + z(1) e^{\phi_{1L}}. \tag{H9}$$

The detailed-balance condition for the rates $p(1j|Li, J)$ and $p(Lj|1i, J), \eta)$ is now broken by the active exponents. Note that the directing function [96,133] is $\mathcal{U}_j(\ell) = -\beta\epsilon_j(\ell) + \ln g_j$.

The constraint of constant flux implies an important assumption that either $0 < J < \nu(L)$ or $0 < -J < \nu(1)$. The value of the Lagrange multiplier η_{1L} can be found once the structure of the energy levels is specified.

APPENDIX I: ACTIVE EXPONENTS

Active exponents, which can be used to express the violation of the detailed-balance relations [Eq. (37)] in nonequilibrium systems, in the continuum limit entail nonconservative forces and amplified fluctuations, e.g., as discussed in Ref. [96, Supplemental Material Sec. 2]. Here we relate this theory to another phenomenon—force-dependent diffusion. To do so, we consider a Thévenin ensemble of active Boltzmann particles, whose motion is enhanced by constant exponents

$$\phi_{m\ell} = \begin{cases} \phi_+ \text{ if } m = \ell + 1, \\ \phi_- \text{ if } m = \ell - 1, \\ 0 \text{ otherwise}, \end{cases} \tag{I1}$$

which can also be decomposed as

$$\phi_\pm = \Phi \pm \beta F dx/2$$

into the symmetric $\phi_+ + \phi_- = 2\Phi$ and asymmetric $\phi_+ - \phi_- = \beta F dx$ parts, where $F dx$ is interpreted as the work done by the force F acting on a particle along the path dx, cf. Eqs. (37) and (51). Then the master equation (G2) reads

$$\dot{\nu}_m = -\kappa \nu_m + k_- \nu_{m+1} + k_+ \nu_{m-1},$$

where $\nu_m(t)$ is the number of particles at the mth lattice and overdot is the time derivative, whereas the rate constants are given by

$$k_\pm = \frac{1}{dt} \frac{e^{\phi_\pm}}{1 + e^{\phi_+} + e^{\phi_-}}, \quad \kappa = k_+ + k_- \frac{1}{dt} \frac{e^{\phi_+} + e^{\phi_-}}{1 + e^{\phi_+} + e^{\phi_-}}.$$

By expanding $\nu_{m\pm1} = \nu_m \pm dx \nu'_m + dx^2 \nu''_m/2$ with prime standing for the spatial derivative, we get

$$\dot{\nu}_m = \frac{\kappa dx^2}{2} \nu''_m - (k_+ - k_-) dx \nu'_m, \tag{I2}$$

in which we used the identity $\kappa = k_+ + k_-$. Then we divide Eq. (I2) by dx and substitute

$$\kappa = \frac{1}{dt} \frac{e^{\frac{\beta F dx}{2}} + e^{-\frac{\beta F dx}{2}}}{e^{-\Phi} + e^{\frac{\beta F dx}{2}} + e^{-\frac{\beta F dx}{2}}} \simeq \frac{2}{dt(2 + e^{-\Phi})},$$

$$k_+ - k_- = \frac{1}{dt} \frac{e^{\frac{\beta F dx}{2}} - e^{-\frac{\beta F dx}{2}}}{e^{-\Phi} + e^{\frac{\beta F dx}{2}} + e^{-\frac{\beta F dx}{2}}} \simeq \frac{\beta F dx}{dt(2 + e^{-\Phi})},$$

where we neglect the terms that would lead to $O(dx^3)$, and take the continuum limit with

$$\lim_{dx \to 0} \frac{dx^2}{dt(2 + e^{-\Phi})} = D(\Phi), \quad \lim_{dx \to 0} \frac{\nu}{dx} = \rho,$$

to obtain the Smoluchowski diffusion equation

$$\partial_t \rho = \nabla \cdot (D(\Phi) \nabla \rho - \beta D(\Phi) \boldsymbol{F}). \tag{I3}$$

The above equations put in evidence the nonconservative force F, and allow us to define an effective temperature $\tilde{\beta}$ by imposing the Einstein relation for the mobility

$\beta D(\Phi) = \tilde{\beta} D(0)$, from which

$$\tilde{\beta} = \frac{\beta D(\Phi)}{D(0)} \sim \frac{3\beta}{2 + \exp(-\Phi)}. \tag{I4}$$

For example, if we assume a simple force $\beta F = \lim_{dx\to 0} \hat{\phi}/dx$, which entails $\Phi = \hat{\phi}/2$, then we may transform Eq. (I3) into

$$\begin{aligned} \partial_t \rho &= \nabla \cdot \left(D(F) \nabla \rho - \beta D(F) \boldsymbol{F} \right) \\ &= \nabla \cdot \left(\frac{\tilde{\beta}(F)}{\beta} D(0) \nabla \rho - \tilde{\beta}(F) D(0) \boldsymbol{F} \right). \end{aligned} \tag{I5}$$

APPENDIX J: SIMULATING A CONSTRAINED MARKOV CHAIN

Under equilibrium conditions, the stochastic process described by Eq. (47) in discrete time can be simulated by using standard computational techniques. Each step of the simulation begins with a given distribution of particles $\boldsymbol{\nu}$. For each lattice site $\ell \in \{1, 2, 3\}$ we generate ν_ℓ pseudorandom numbers $u_i(\ell)$ with $i = 1, 2, ..., \nu_\ell$, which are uniformly distributed on the unit interval, i.e., $u_i(\ell) \in I = [0, 1)$. Iterating over each site ℓ, we make partitions $I_m(\ell = 1, 2, 3)$ of the interval I into three *bins* $m = 1, 2, 3$ of size $p_{m\ell}$. Then, as if constructing a histogram, we determine the number of particles $n_{m\ell} = \#[u_i(\ell) \in I_m(\ell)]$ which are transferred from the site ℓ into the site m. The result of the simulation step is a new state $\boldsymbol{\nu}'$ with components $\nu'_m = \sum_{\ell=1}^{3} n_{m\ell}$.

The described algorithm is also applicable in nonequilbirium simulations without explicit constraints, as in the case 3 of Sec. IV, since the matrix $\boldsymbol{p}$ remains invariant at all steps. However, to restrict the sampled numbers $n_{m\ell}$ in a certain way, we need to modify this algorithm.

First we discuss the simplest modification of the algorithm, which is necessary for simulating the directed motion of self-propelling particles (Sec. III)—case 4 considered in Sec. IV. Specifically, to ensure that in each step of the simulation $\sum_{\ell=1}^{3} n_{\ell+1,\ell} = J_{\rm DM}$, we adjust the boundaries of the bins $I_m(\ell)$ as follows. First we order these bins so that $I_{\ell+1}(\ell)$ is the left-most subinterval in each partitioning of I, i.e.,

$$\forall u \in I_{\ell+1}(\ell), u' \in I_{m\neq\ell+1}(\ell) : u < u'.$$

Ordering of the other subintervals does not matter.

Then we pull all randomly generated numbers $u_i(\ell)$ together into a single sample

$$\boldsymbol{U} = \cup_{\ell=1,i=1}^{3,\nu_\ell} \{u_i(\ell)\}.$$

Because all elements of the form

$$p_{\ell+1,\ell}(\eta_{\rm DM}) = p_+(\eta_{\rm DM}) = (1 + 2e^{\eta_{\rm DM}})^{-1}, \tag{J1}$$

which determine the size of the bins $I_{\ell+1}(\ell)$, are equal, the number of elements

$$\#[U_i \in \boldsymbol{U} : U_i < p_+(\eta_{\rm DM})]$$

counts the total number of particles jumping to the right from any site $\ell \in \{1, 2, 3\}$. So we may choose such $\eta_{\rm DM}$, that the interval $I_+(\eta_{\rm DM}) = [0, p_+)$ of size p_+ contains precisely $J_{\rm DM}$ numbers $U_i \in \boldsymbol{U}$:

$$\#[u \in \boldsymbol{U} \cap I_+(\eta_{\rm DM})] = J_{\rm DM}. \tag{J2}$$

In practice there is an interval of values $\eta_{\rm DM} \in \hat{I}$ that satisfy Eq. (J2). This interval becomes narrower as the total number of particles increases $N \to \infty$. Therefore, if we sort numbers $U(i = 1, 2, ..., N) \in \boldsymbol{U}$ in the increasing order, that is $U_i < U_{i+1}$, then we may estimate

$$\eta_{\rm DM} = -\ln[2p_+/(1 - p_+)],$$

with

$$p_+ = [U(J_{\rm DM}) + U(J_{\rm DM} + 1)]/2.$$

The described algorithm imposing a constant cumulative flux $J_{\rm DM}$ can be easily adapted to the simulations under the constraint of cumulative displacement $J_{\rm AD}$ (case 5 in Sec. IV). Requiring $J_{\rm AD}$ particles out of the total N to move is equivalent to fixing the number $J_0 = N - J_{\rm AD}$ to remain at the same site in each step. Therefore we reorder this time intervals $I_m(\ell)$, so that $I_\ell(\ell)$ is the left-most in the partitioning scheme. Noting that all the elements

$$p_{\ell\ell}(\eta_{\rm AD}) = p_0(\eta_{\rm AD}) = (1 + 2e^{-\eta_{\rm AD}})^{-1} \tag{J3}$$

are equal, we obtain

$$\eta_{\rm AD} = \ln[2p_0/(1 - p_0)],$$

with

$$p_0 = [U(J_0) + U(J_0 + 1)]/2.$$

Modifications of the algorithm, which are required to simulate the system with a constant boundary flux (case 2 in Sec. IV), are more complicated. We focus on the transition probabilities

$$p_{1L} = (2e^{\eta} + 1)^{-1}, \quad p_{L1} = (2e^{-\eta} + 1)^{-1}, \tag{J4}$$

which can be related by

$$p(\eta) = p_{1L}(\eta) = \frac{1 - p_{L1}(\eta)}{1 + 3p_{L1}(\eta)}.$$

Note that as the probability of particles jumping from the site L to 1 vanishes, $p(\eta) \to 0$, all the particles at the site 1 transit to L in one simulation step. Thereby we observe the most negative possible flux $J_{\rm min} = -\nu_1$. As the probability $p(\eta) \to 1$, we observe the largest possible flux $J_{\rm max} = \nu_3$.

Now we merge the samples $u_i(1)$ and $u_i(L)$ from the first and third sites as

$$\boldsymbol{\Upsilon} = \cup_{i=1}^{\nu_1} \left\{ \frac{1 - u_i(1)}{1 + 3u_i(1)} \right\} \cup_{i=1}^{\nu_3} \{u_i(3)\},$$

and order them in the increasing order $\Upsilon(i) < \Upsilon(i + 1)$. Finally, we choose $\eta = -\ln[2p/(1 - p)]$ with

$$p = \frac{\Upsilon(J - J_{\rm min}) + \Upsilon(J - J_{\rm min} + 1)}{2}.$$

[1] C. M. Kriebisch, O. Bantysh, L. Baranda Pellejero, A. Belluati, E. Bertosin, K. Dai, M. de Roy, H. Fu, N. Galvanetto, J. M. Gibbs, S. S. Gomez, G. Granatelli, A. Griffo, M. Guix, C. O. Gurdap, J. Harth-Kitzerow, I. S. Haugerud, G. Häfner, P. Jaiswal, S. Javed, *et al.*, A roadmap toward the synthesis of life, Chem **11**, 102399 (2025).

[2] A. Genthon, C. D. Modes, F. Jülicher, and S. W. Grill, Nonequilibrium transitions in a template copying ensemble, Phys. Rev. Lett. **134**, 068402 (2025).

[3] I. S. Haugerud, P. Jaiswal, and C. A. Weber, Nonequilibrium wet–dry cycling acts as a catalyst for chemical reactions, J. Phys. Chem. B **128**, 1724 (2024).

[4] Y. Wang, E. Lei, Y.-H. Ma, Z. C. Tu, and G. Li, Thermodynamic geometric control of active matter, Phys. Rev. E **112**, 054124 (2025).

[5] J. Bauermann, S. Laha, P. M. McCall, F. Jülicher, and C. A. Weber, Chemical kinetics and mass action in coexisting phases, J. Am. Chem. Soc. **144**, 19294 (2022).

[6] J. Bauermann, G. Bartolucci, J. Boekhoven, C. A. Weber, and F. Jülicher, Formation of liquid shells in active droplet systems, Phys. Rev. Res. **5**, 043246 (2023).

[7] Z.-K. Liu, Thermodynamics and its prediction and calphad modeling: Review, state of the art, and perspectives, Calphad **82**, 102580 (2023).

[8] R. Zakine and E. Vanden-Eijnden, Minimum-action method for nonequilibrium phase transitions, Phys. Rev. X **13**, 041044 (2023).

[9] M. J. Bowick, N. Fakhri, M. C. Marchetti, and S. Ramaswamy, Symmetry, thermodynamics, and topology in active matter, Phys. Rev. X **12**, 010501 (2022).

[10] T. Markovich, E. Fodor, E. Tjhung, and M. E. Cates, Thermodynamics of active field theories: Energetic cost of coupling to reservoirs, Phys. Rev. X **11**, 021057 (2021).

[11] P. Gaspard and R. Kapral, Active matter, microreversibility, and thermodynamics, Research **2020**, 9739231 (2020).

[12] T. Herpich, J. Thingna, and M. Esposito, Collective power: Minimal model for thermodynamics of nonequilibrium phase transitions, Phys. Rev. X **8**, 031056 (2018).

[13] P. Sartori and S. Leibler, Lessons from equilibrium statistical physics regarding the assembly of protein complexes, Proc. Natl. Acad. Sci. USA **117**, 114 (2019).

[14] F. Benoist and P. Sartori, High-speed combinatorial polymerization through kinetic-trap encoding, Phys. Rev. Lett. **134**, 038402 (2025).

[15] S. C. Takatori and J. F. Brady, Towards a thermodynamics of active matter, Phys. Rev. E **91**, 032117 (2015).

[16] R. Chetrite and H. Touchette, Nonequilibrium Markov processes conditioned on large deviations, Ann. Henri Poincaré **16**, 2005 (2015).

[17] N. Freitas, J.-C. Delvenne, and M. Esposito, Stochastic thermodynamics of nonlinear electronic circuits: A realistic framework for computing around kT, Phys. Rev. X **11**, 031064 (2021).

[18] N. I. Petridou, B. Corominas-Murtra, C.-P. Heisenberg, and E. Hannezo, Rigidity percolation uncovers a structural basis for embryonic tissue phase transitions, Cell **184**, 1914 (2021).

[19] E. Tang and R. Golestanian, Quantifying configurational information for a stochastic particle in a flow-field, New J. Phys. **22**, 083060 (2020).

[20] E. Tang, J. Agudo-Canalejo, and R. Golestanian, Topology protects chiral edge currents in stochastic systems, Phys. Rev. X **11**, 031015 (2021).

[21] Y. I. Li, R. Garcia-Millan, M. E. Cates, and E. Fodor, Towards a liquid-state theory for active matter (a), Europhys. Lett. **142**, 57004 (2023).

[22] F. Avanzini, T. Aslyamov, E. Fodor, and M. Esposito, Nonequilibrium thermodynamics of non-ideal reaction–diffusion systems: Implications for active self-organization, J. Chem. Phys. **161**, 174108 (2024).

[23] C. Zheng and E. Tang, A topological mechanism for robust and efficient global oscillations in biological networks, Nat. Commun. **15**, 6453 (2024).

[24] A. Raghu and I. Neri, Effective affinity for generic currents in Markov processes, J. Stat. Phys. **192**, 50 (2025).

[25] G. Tkačik and P. R. T. Wolde, Information processing in biochemical networks, Annu. Rev. Biophys. **54**, 249 (2025).

[26] C. Maes, Frenesy: Time-symmetric dynamical activity in nonequilibria, Phys. Rep. **850**, 1 (2020).

[27] C. Maes, Local detailed balance, SciPost Phys. Lect. Notes **32** (2021).

[28] R. M. L. Evans, Detailed balance has a counterpart in nonequilibrium steady states, J. Phys. A: Math. Gen. **38**, 293 (2005).

[29] G. Falasco and M. Esposito, Macroscopic stochastic thermodynamics, Rev. Mod. Phys. **97**, 015002 (2025).

[30] H. Touchette, Introduction to dynamical large deviations of Markov processes, Physica A **504**, 5 (2018).

[31] H. Touchette and R. J. Harris, Large deviation approach to nonequilibrium systems, in *Nonequilibrium Statistical Physics of Small Systems: Fluctuation Relations and Beyond*, edited by R. Klages, W. Just, and C. Jarzynski (Wiley, New York, 2013).

[32] E. Smith, Large-deviation principles, stochastic effective actions, path entropies, and the structure and meaning of thermodynamic descriptions, Rep. Prog. Phys. **74**, 046601 (2011).

[33] H. Touchette, The large deviation approach to statistical mechanics, Phys. Rep. **478**, 1 (2009).

[34] M. Hofer, J. Korbel, R. Hanel, and S. Thurner, Thermodynamics of driven systems with explicitly broken detailed balance, arXiv:2501.12192.

[35] P. Gaspard, Multivariate fluctuation relations for currents, New J. Phys. **15**, 115014 (2013).

[36] D. Ruelle, A review of linear response theory for general differentiable dynamical systems, Nonlinearity **22**, 855 (2009).

[37] J. Schnakenberg, Network theory of microscopic and macroscopic behavior of master equation systems, Rev. Mod. Phys. **48**, 571 (1976).

[38] K. Ghosh, P. D. Dixit, L. Agozzino, and K. A. Dill, The maximum caliber variational principle for nonequilibria, Annu. Rev. Phys. Chem. **71**, 213 (2020).

[39] P. Pradhan, C. P. Amann, and U. Seifert, Nonequilibrium steady states in contact: Approximate thermodynamic structure and zeroth law for driven lattice gases, Phys. Rev. Lett. **105**, 150601 (2010).

[40] A. Porporato and L. Rondoni, Deterministic engines extending Helmholtz thermodynamics, Physica A **640**, 129700 (2024).

[41] F. Cardin and M. Favretti, On the Helmholtz-Boltzmann thermodynamics of mechanical systems, Continuum Mech. Thermodyn. **16**, 15 (2004).
[42] M. Ding and M. E. Cates, Hamiltonian heat baths, coarse-graining and irreversibility: A microscopic dynamical entropy from classical mechanics, arXiv:2503.11334.
[43] S. Caruso, C. Giberti, and L. Rondoni, Dissipation function: Nonequilibrium physics and dynamical systems, Entropy **22**, 835 (2020).
[44] A. Dhar and H. Spohn, Fourier's law based on microscopic dynamics, Comptes Rendus. Phys. **20**, 393 (2019).
[45] A. Agarwal, J. Zhu, C. Hartmann, H. Wang, and L. D. Site, Molecular dynamics in a grand ensemble: Bergmann–Lebowitz model and adaptive resolution simulation, New J. Phys. **17**, 083042 (2015).
[46] D. Ruelle, A mechanical model for Fourier's law of heat conduction, Commun. Math. Phys. **311**, 755 (2012).
[47] J. L. Lebowitz and P. G. Bergmann, Irreversible Gibbsian ensembles, Ann. Phys. **1**, 1 (1957).
[48] P. G. Bergmann and J. L. Lebowitz, New approach to nonequilibrium processes, Phys. Rev. **99**, 578 (1955).
[49] J. Gibbs, *Elementary Principles in Statistical Mechanics: Developed with Especial Reference to the Rational Foundations of Thermodynamics* (C. Scribner's Sons, New York, NY, 1902).
[50] H. Callen, *Thermodynamics and an Introduction to Thermostatistics* (Wiley, New York, NY, 1991).
[51] M. Esposito, Stochastic thermodynamics under coarse graining, Phys. Rev. E **85**, 041125 (2012).
[52] A. Puglisi, S. Pigolotti, L. Rondoni, and A. Vulpiani, Entropy production and coarse graining in Markov processes, J. Stat. Mech.: Theory Exp. (2010) P05015.
[53] P. E. Harunari, A. Dutta, M. Polettini, and E. Roldán, What to learn from a few visible transitions' statistics? Phys. Rev. X **12**, 041026 (2022).
[54] B. Altaner and J. Vollmer, Fluctuation-preserving coarse graining for biochemical systems, Phys. Rev. Lett. **108**, 228101 (2012).
[55] E. T. Jaynes, The minimum entropy production principle, Annu. Rev. Phys. Chem. **31**, 579 (1980).
[56] E. T. Jaynes, Information theory and statistical mechanics, Phys. Rev. **106**, 620 (1957).
[57] A. A. Filyukov and V. Y. Karpov, Description of steady transport processes by the method of the most probable path of evolution, J. Eng. Phys. **13**, 326 (1967).
[58] A. A. Filyukov and V. Y. Karpov, Method of the most probable path of evolution in the theory of stationary irreversible processes, J. Eng. Phys. **13**, 416 (1967).
[59] P. Attard, The second entropy: A general theory for non-equilibrium thermodynamics and statistical mechanics, Annu. Rep. Sect. C **105**, 63 (2009).
[60] P. Attard, *Non-Equilibrium Thermodynamics and Statistical Mechanics: Foundations and Applications* (Oxford University Press, Oxford, UK, 2012).
[61] A. A. Filyukov, Compatibility property of steady systems, J. Eng. Phys. **14**, 429 (1968).
[62] H. Haken, A new access to path integrals and Fokker Planck equations via the maximum calibre principle, Z. Phys. B **63**, 505 (1986).
[63] R. Dewar, Information theory explanation of the fluctuation theorem, maximum entropy production and self-organized criticality in non-equilibrium stationary states, J. Phys. A: Math. Gen. **36**, 631 (2003).
[64] P. Gaspard, Time-reversed dynamical entropy and irreversibility in Markovian random processes, J. Stat. Phys. **117**, 599 (2004).
[65] R. C. Dewar, Maximum entropy production and the fluctuation theorem, J. Phys. A: Math. Gen. **38**, L371 (2005).
[66] K. Ghosh, K. A. Dill, M. M. Inamdar, E. Seitaridou, and R. Phillips, Teaching the principles of statistical dynamics, Am. J. Phys. **74**, 123 (2006).
[67] V. Lecomte, C. Appert-Rolland, and F. van Wijland, Thermodynamic formalism for systems with Markov dynamics, J. Stat. Phys. **127**, 51 (2007).
[68] E. Seitaridou, M. M. Inamdar, R. Phillips, K. Ghosh, and K. Dill, Measuring flux distributions for diffusion in the small-numbers limit, J. Phys. Chem. B **111**, 2288 (2007).
[69] D. Wu, K. Ghosh, M. Inamdar, H. J. Lee, S. Fraser, K. Dill, and R. Phillips, Trajectory approach to two-state kinetics of single particles on sculpted energy landscapes, Phys. Rev. Lett. **103**, 050603 (2009).
[70] M. Otten and G. Stock, Maximum caliber inference of nonequilibrium processes, J. Chem. Phys. **133**, 034119 (2010).
[71] G. Stock, K. Ghosh, and K. A. Dill, Maximum caliber: A variational approach applied to two-state dynamics, J. Chem. Phys. **128**, 194102 (2008).
[72] S. Pressé, K. Ghosh, R. Phillips, and K. A. Dill, Dynamical fluctuations in biochemical reactions and cycles, Phys. Rev. E **82**, 031905 (2010).
[73] C. Monthus, Non-equilibrium steady states: maximization of the Shannon entropy associated with the distribution of dynamical trajectories in the presence of constraints, J. Stat. Mech.: Theory Exp. (2011) P03008.
[74] H. Ge, S. Pressé, K. Ghosh, and K. A. Dill, Markov processes follow from the principle of maximum caliber, J. Chem. Phys. **136**, 064108 (2012).
[75] S. Pressé, K. Ghosh, and K. A. Dill, Modeling stochastic dynamics in biochemical systems with feedback using maximum caliber, J. Phys. Chem. B **115**, 6202 (2011).
[76] K. Ghosh, Stochastic dynamics of complexation reaction in the limit of small numbers, J. Chem. Phys. **134**, 195101 (2011).
[77] J. Lee and S. Pressé, A derivation of the master equation from path entropy maximization, J. Chem. Phys. **137**, 074103 (2012).
[78] J. Lee and S. Pressé, Microcanonical origin of the maximum entropy principle for open systems, Phys. Rev. E **86**, 041126 (2012).
[79] S. Pressé, K. Ghosh, J. Lee, and K. A. Dill, Principles of maximum entropy and maximum caliber in statistical physics, Rev. Mod. Phys. **85**, 1115 (2013).
[80] M. J. Hazoglou, V. Walther, P. D. Dixit, and K. A. Dill, Communication: Maximum caliber is a general variational principle for nonequilibrium statistical mechanics, J. Chem. Phys. **143**, 051104 (2015).
[81] G. Auletta, L. Rondoni, and A. Vulpiani, On the relevance of the maximum entropy principle in non-equilibrium statistical mechanics, Eur. Phys. J.: Spec. Top. **226**, 2327 (2017).
[82] S. Chibbaro, L. Rondoni, and A. Vulpiani, *Reductionism, Emergence and Levels of Reality: The Importance of Being Borderline* (Springer International Publishing, Berlin, 2014).

[83] M. Tuckerman, *Statistical Mechanics: Theory and Molecular Simulation* (Oxford University Press, Oxford, UK, 2023).
[84] E. M. Pearson, T. Halicioglu, and W. A. Tiller, Laplace-transform technique for deriving thermodynamic equations from the classical microcanonical ensemble, Phys. Rev. A **32**, 3030 (1985).
[85] R. M. L. Evans, Rules for transition rates in nonequilibrium steady states, Phys. Rev. Lett. **92**, 150601 (2004).
[86] R. Evans, Driven steady states: Rules for transition rates, Physica A **340**, 364 (2004).
[87] J. A. Pachter and K. A. Dill, Nonequilibrium statistical physics beyond the ideal heat bath approximation, Phys. Rev. E **107**, 014131 (2023).
[88] J. Rombouts, J. Elliott, and A. Erzberger, Forceful patterning: Theoretical principles of mechanochemical pattern formation, EMBO Rep. **24**, e57739 (2023).
[89] J. A. Davies and F. Glykofrydis, Engineering pattern formation and morphogenesis, Biochem. Soc. Trans. **48**, 1177 (2020).
[90] D. Hua, R. Xiong, K. Braeckmans, B. Scheid, C. Huang, F. Sauvage, and S. C. De Smedt, Concentration gradients in material sciences: Methods to design and biomedical applications, Adv. Funct. Mater. **31**, 2009005 (2021).
[91] J. Halatek and E. Frey, Rethinking pattern formation in reaction–diffusion systems, Nat. Phys. **14**, 507 (2018).
[92] L. M. R. Keil, F. M. Möller, M. Kieß, P. W. Kudella, and C. B. Mast, Proton gradients and pH oscillations emerge from heat flow at the microscale, Nat. Commun. **8**, 1897 (2017).
[93] J. R. Manning, Diffusion in a chemical concentration gradient, Phys. Rev. **124**, 470 (1961).
[94] K. Sharp and F. Matschinsky, Translation of Ludwig Boltzmann's paper "On the relationship between the second fundamental theorem of the mechanical theory of heat and probability calculations regarding the conditions for thermal equilibrium" sitzungberichte der kaiserlichen akademie der wissenschaften. Mathematisch-naturwissen classe. Abt. II, LXXVI 1877, pp. 373–435 (Wien. Ber. 1877, 76:373-435). Reprinted in Wiss. Abhandlungen, Vol. II, reprint 42, p. 164–223, Barth, Leipzig, 1909, Entropy **17**, 1971 (2015).
[95] A. H. Carter, *Classical and Statistical Thermodynamics* (Pearson, Upper Saddle River, NJ, 2001).
[96] R. Belousov, S. Savino, P. Moghe, T. Hiiragi, L. Rondoni, and A. Erzberger, Poissonian cellular Potts models reveal nonequilibrium kinetics of cell sorting, Phys. Rev. Lett. **132**, 248401 (2024).
[97] M. Kardar, *Statistical Physics of Particles* (Cambridge University Press, Cambridge, UK, 2007).
[98] P. J. Flory, Thermodynamics of high polymer solutions, J. Chem. Phys. **10**, 51 (1942).
[99] M. L. Huggins, Some properties of solutions of long-chain compounds. J. Phys. Chem. **46**, 151 (1942).
[100] C. A. Weber, D. Zwicker, F. Jülicher, and C. F. Lee, Physics of active emulsions, Rep. Prog. Phys. **82**, 064601 (2019).
[101] S. Safran, *Statistical Thermodynamics of Surfaces, Interfaces, and Membranes* (CRC Press, Boca Raton, FL, 2018).
[102] S. Katz, J. L. Lebowitz, and H. Spohn, Nonequilibrium steady states of stochastic lattice gas models of fast ionic conductors, J. Stat. Phys. **34**, 497 (1984).
[103] D. A. Wolf-Gladrow, *Lattice Gas Cellular Automata and Lattice Boltzmann Models* (Springer, Berlin, Heidelberg, 2000).
[104] S. A. Janowsky and J. L. Lebowitz, Finite-size effects and shock fluctuations in the asymmetric simple-exclusion process, Phys. Rev. A **45**, 618 (1992).
[105] B. Derrida, An exactly soluble non-equilibrium system: The asymmetric simple exclusion process, Phys. Rep. **301**, 65 (1998).
[106] O. Golinelli and K. Mallick, The asymmetric simple exclusion process: An integrable model for non-equilibrium statistical mechanics, J. Phys. A: Math. Gen. **39**, 12679 (2006).
[107] T. Chou, K. Mallick, and R. K. P. Zia, Non-equilibrium statistical mechanics: From a paradigmatic model to biological transport, Rep. Prog. Phys. **74**, 116601 (2011).
[108] M. R. Hilário, D. Kious, and A. Teixeira, Random walk on the simple symmetric exclusion process, Commun. Math. Phys. **379**, 61 (2020).
[109] J. Elliott, H. Shah, R. Belousov, G. Dey, and A. Erzberger, Repulsive particle interactions enable selective information processing at cellular interfaces, Phys. Rev. Lett. **135**, 218403 (2025).
[110] H. J. Bowlden, Detailed balance in nonvertical transitions, J. Phys. Chem. Solids **3**, 115 (1957).
[111] T. S. Nguyen, R. Nanguneri, and J. Parkhill, How electronic dynamics with Pauli exclusion produces Fermi-Dirac statistics, J. Chem. Phys. **142**, 134113 (2015).
[112] S. De Groot and P. Mazur, *Non-Equilibrium Thermodynamics*, Dover Books on Physics (Dover Publications, Mineola, NY, 2013).
[113] C. Bechinger, R. Di Leonardo, H. Löwen, C. Reichhardt, G. Volpe, and G. Volpe, Active particles in complex and crowded environments, Rev. Mod. Phys. **88**, 045006 (2016).
[114] A. Svetlov, M. Vasiliev, E. Kononov, O. Petrov, and F. Trukhachev, 3D active Brownian motion of single dust particles induced by a laser in a DC glow discharge, Molecules **28**, 1790 (2023).
[115] K. J. M. Bishop, S. L. Biswal, and B. Bharti, Active colloids as models, materials, and machines, Annu. Rev. Chem. Biomol. Eng. **14**, 1 (2023).
[116] B. Kavčič and G. Tkačik, Token-driven totally asymmetric simple exclusion processes, Phys. Rev. E **111**, 054122 (2025).
[117] L. Abbaspour and S. Klumpp, Enhanced diffusion of a tracer particle in a lattice model of a crowded active system, Phys. Rev. E **103**, 052601 (2021).
[118] L. Meng, Y. Jin, Y. Guan, J. Xu, and J. Lin, Diffusion enhancement in bacterial cytoplasm through an active random force, Phys. Rev. Res. **5**, L032018 (2023).
[119] D. J. Evans and J. F. Ely, Viscous flow in the stress ensemble, Mol. Phys. **59**, 1043 (1986).
[120] F. Müller-Plathe, Reversing the perturbation in nonequilibrium molecular dynamics: An easy way to calculate the shear viscosity of fluids, Phys. Rev. E **59**, 4894 (1999).
[121] R. Chetrite and H. Touchette, Nonequilibrium microcanonical and canonical ensembles and their equivalence, Phys. Rev. Lett. **111**, 120601 (2013).
[122] D. Evans and G. Morriss, *Statistical Mechanics of Nonequilibrium Liquids*, DOAB Directory of Open Access Books (ANU Press, Canberra, Australia, 2007).
[123] B. N. Miller and P. M. Larson, Heat flow in a linear harmonic chain: An information-theoretic approach to the nonequilibrium stationary state, Phys. Rev. A **20**, 1717 (1979).

[124] A. Kato and D. Jou, Breaking of equipartition in one-dimensional heat-conducting systems, Phys. Rev. E **64**, 052201 (2001).

[125] L. Conti, P. D. Gregorio, G. Karapetyan, C. Lazzaro, M. Pegoraro, M. Bonaldi, and L. Rondoni, Effects of breaking vibrational energy equipartition on measurements of temperature in macroscopic oscillators subject to heat flux, J. Stat. Mech.: Theory Exp. (2013) P12003.

[126] B. Hille, Ionic channels in excitable membranes. Current problems and biophysical approaches, Biophys. J. **22**, 283 (1978).

[127] Q. Ren, Q. Cui, K. Chen, J. Xie, and P. Wang, Salinity-gradient power harvesting using osmotic energy conversion with designed interfacial nanostructures under thermal modulation, Desalination **535**, 115802 (2022).

[128] P. S. Senanayake, A. Lugo, M. F. Ahmed, Z. Stoll, N. E. Moe, J. Barber, W. Shane Walker, P. Xu, and H. Wang, Electrodialysis modeling for desalination and resource recovery, Curr. Opin. Chem. Eng. **47**, 101081 (2025).

[129] Source code, which implements numerical simulations in Sec. IV, is available at https://git.embl.de/rbelouso/microcaliber.

[130] U. Seifert, Stochastic thermodynamics, fluctuation theorems and molecular machines, Rep. Prog. Phys. **75**, 126001 (2012).

[131] L. Peliti and S. Pigolotti, *Stochastic Thermodynamics: An Introduction* (Princeton University Press, Princeton, NJ, 2021).

[132] R. Belousov, M. N. Qaisrani, A. Hassanali, and E. Roldán, First-passage fingerprints of water diffusion near glutamine surfaces, Soft Matter **16**, 9202 (2020).

[133] R. Belousov, A. Hassanali, and E. Roldán, Statistical physics of inhomogeneous transport: Unification of diffusion laws and inference from first-passage statistics, Phys. Rev. E **106**, 014103 (2022).

[134] S. Chandrasekhar, Stochastic problems in physics and astronomy, Rev. Mod. Phys. **15**, 1 (1943).

[135] Z. Burda, J. Duda, J. M. Luck, and B. Waclaw, Localization of the maximal entropy random walk, Phys. Rev. Lett. **102**, 160602 (2009).

[136] P. D. Dixit and K. A. Dill, Inferring microscopic kinetic rates from stationary state distributions, J. Chem. Theory Comput. **10**, 3002 (2014).

[137] P. D. Dixit, Stationary properties of maximum-entropy random walks, Phys. Rev. E **92**, 042149 (2015).

[138] B. Bijnens and C. Maes, Pushing run-and-tumble particles through a rugged channel, J. Stat. Mech.: Theory Exp. (2021) 033206.

[139] R. C. Tolman, *The Principles of Statistical Mechanics* (Courier Corporation, North Chelmsford, MA, 1979).

[140] G. Gallavotti, *Statistical Mechanics: A Short Treatise* (Springer Science & Business Media, Cham, 1999).

[141] D. J Evans and G. P Morriss, *Statistical Mechanics of Nonequilbrium Liquids* (ANU Press, Canberra, Australia, 2007).

[142] D. J. Evans, E. G. D. Cohen, and G. P. Morriss, Probability of second law violations in shearing steady states, Phys. Rev. Lett. **71**, 2401 (1993).

[143] D. J. Evans, S. R. Williams, D. J. Searles, and L. Rondoni, On typicality in nonequilibrium steady states, J. Stat. Phys. **164**, 842 (2016).

[144] W. G. Hoover, Nonequilibrium molecular dynamics, in *Molecular Dynamics*, edited by H. Araki, J. Ehlers, K. Hepp, H. A. Weidenmüller, and J. Zittartz, Lecture Notes in Physics Vol. 258 (Springer, Berlin, Germany, 1986), p. 92.

[145] B. Hafskjold, T. Ikeshoji, and S. K. Ratkje, On the molecular mechanism of thermal diffusion in liquids, Mol. Phys. **80**, 1389 (1993).

[146] F. Müller-Plathe, A simple nonequilibrium molecular dynamics method for calculating the thermal conductivity, J. Chem. Phys. **106**, 6082 (1997).

[147] H. Haken, Application of the maximum information entropy principle to selforganizing systems, Z. Phys. B **61**, 335 (1985).

[148] H. Haken, The maximum entropy principle for nonequilibrium phase transitions: Determination of order parameters, slaved modes, and emerging patterns, Z. Phys. B **63**, 487 (1986).

[149] J. E. Mayer and E. Montroll, Molecular distribution, J. Chem. Phys. **9**, 2 (1941).